



Mass Spectrometric Characterization of HSV-1 L-Particles From Human Dendritic Cells and BHK21 Cells and Analysis of Their Functional Role

OPEN ACCESS

Edited by:

Akio Adachi,
Department of Microbiology, Kansai
Medical University, Japan

Reviewed by:

Russell Diefenbach,
Faculty of Medicine and Health
Sciences, Macquarie University,
Australia
Roger Lippé,
Université de Montréal, Canada
Gill Elliott,
University of Surrey, United Kingdom

*Correspondence:

Alexander Steinkasserer
alexander.steinkasserer@
uk-erlangen.de
Linda Popella
linda.grosche@uk-erlangen.de;
linda_gro@web.de

Specialty section:

This article was submitted to
Virology,
a section of the journal
Frontiers in Microbiology

Received: 03 April 2020

Accepted: 28 July 2020

Published: 29 September 2020

Citation:

Birzer A, Kraner ME,
Heilingloh CS, Mühl-Zürbes P,
Hofmann J, Steinkasserer A and
Popella L (2020) Mass Spectrometric
Characterization of HSV-1 L-Particles
From Human Dendritic Cells
and BHK21 Cells and Analysis
of Their Functional Role.
Front. Microbiol. 11:1997.
doi: 10.3389/fmicb.2020.01997

**Alexandra Birzer¹, Max Edmund Kraner², Christiane Silke Heilingloh³,
Petra Mühl-Zürbes¹, Jörg Hofmann², Alexander Steinkasserer^{1*} and Linda Popella^{1*}**

¹ Department of Immune Modulation, Universitätsklinikum Erlangen, Erlangen, Germany, ² Division of Biochemistry, Department of Biology, Friedrich-Alexander Universität Erlangen-Nürnberg, Erlangen, Germany, ³ Department of Infectious Diseases, University Hospital Essen, University of Duisburg-Essen, Essen, Germany

Herpes simplex virus type 1 (HSV-1) is a very common human pathogenic virus among the world's population. The lytic replication cycle of HSV-1 is, amongst others, characterized by a tripartite viral gene expression cascade, the assembly of nucleocapsids involving their subsequent nuclear egress, tegumentation, re-envelopment and the final release of progeny viral particles. During productive infection of a multitude of different cell types, HSV-1 generates not only infectious heavy (H-) particles, but also non-infectious light (L-) particles, lacking the capsid. In monocyte-derived mature dendritic cells (mDCs), HSV-1 causes a non-productive infection with the predominant release of L-particles. Until now, the generation and function of L-particles is not well understood, however, they are described as factors transferring viral components to the cellular microenvironment. To obtain deeper insights into the L-particle composition, we performed a mass-spectrometry-based analysis of L-particles derived from HSV-1-infected mDCs or BHK21 cells and H-particles from the latter one. In total, we detected 63 viral proteins in both H- and L-particle preparations derived from HSV-1-infected BHK21 cells. In L-particles from HSV-1-infected mDCs we identified 41 viral proteins which are differentially distributed compared to L-particles from BHK21 cells. In this study, we present data suggesting that L-particles modify mDCs and suppress their T cell stimulatory capacity. Due to the plethora of specific viral proteins incorporated into and transmitted by L-particles, it is tempting to speculate that L-particles manipulate non-infected bystander cells for the benefit of the virus.

Keywords: HSV-1, mass spectrometry, heavy particles, light particles, BHK21 cells, dendritic cells, T cell stimulation, immunomodulatory effect

Abbreviations: BHK, baby hamster kidney; ICP, infected cell protein; RT, room temperature; UL, unique long; US, unique short.

INTRODUCTION

The human pathogenic herpes simplex virus type 1 (HSV-1) represents the prototype of the α -herpesvirus subfamily. In contrast to the highly diverse and complex herpesvirus-associated diseases, herpesviruses share a conserved genome composition and virion morphology (Whitley and Griffiths, 2002; Schleiss, 2009; Watson et al., 2012). Common among all herpesviruses, HSV-1 consists of the viral DNA genome surrounded by a multi protein layer, known as tegument, and the outer glycoprotein rich host-derived membrane, forming the envelope (Laine et al., 2015).

After attachment to and penetrating the cell, viral tegument proteins play an essential role in modulating the infected cells for the benefit of the virus. Furthermore, specific tegument proteins enter the nucleus and support the initiation of the tripartite gene expression cascade divided into immediate-early (IE), early (E) and late (L) gene expression (Guo et al., 2010). In particular, the tegument proteins ICP0, ICP4, and VP16 are released into the cell and facilitate initiation of the gene expression cascade. Simultaneously, the virion host shutoff protein (vhs) destabilizes cellular mRNAs to, e.g., hamper the host's immune response against HSV-1 (Taddeo et al., 2010; Dauber et al., 2014). After completion of the viral *de novo* protein synthesis, HSV-1 progeny capsids are assembled inside the nucleus and subsequently cross the nuclear membrane bilayer getting enveloped and de-enveloped at the inner nuclear membrane (INM, primary envelopment) and the outer nuclear membrane (ONM), respectively (Mettenleiter, 2002; Johnson and Baines, 2011; Crump, 2018). Primary envelopment and following de-envelopment in the perinuclear space requires the multiprotein nuclear egress complex (NEC), composed of the viral proteins UL31 and UL34 (Reynolds et al., 2002; Bigalke and Heldwein, 2017). Having passed the nuclear membrane, capsids get coated with tegument proteins by a step called tegumentation (Vittone et al., 2005; Henaff et al., 2013). In a last step, virions bud of cytoplasmic membranes, such as derived from the trans-Golgi network or endosomes, providing the lipid envelope of mature virions (secondary envelopment) for the subsequent release (Lv et al., 2019). Apart from mature infectious virions, so-called heavy (H-) particles, a lytic HSV-1 infection will also give rise to the production of light (L-) particles, which are void of the capsid and thus are not infectious (Hogue et al., 2016).

HSV-1 has established well elaborated strategies to efficiently infect and replicate in a variety of different cell types as well as several host species (Karasneh and Shukla, 2011). Apart from initially infected cells during a primary HSV-1 infection in, e.g., fibroblasts or epithelial cells, also immune cells, such as dendritic cells (DCs) can be infected (Smiley et al., 1985; Goldwich et al., 2011). DCs operate at the interface of the innate and adaptive immune system by presenting peripheral antigens to T cells for their activation, hence serving as promising targets for HSV-1-mediated immune modulations. In the last decades, several immune evasion mechanisms of HSV-1 regarding DC surface protein expression, migration, maturation and T cell stimulation have been deciphered (Kruse et al., 2000; Pollara

et al., 2003; Prechtel et al., 2005; Theodoridis et al., 2011; Heilingloh et al., 2015).

Recent observations by Turan et al. revealed that HSV-1 exploits autophagic turnover to degrade nuclear lamins in immature DCs (iDCs), facilitating nuclear egress of viral capsids and thus virion assembly (Turan et al., 2019). By contrast to their immature counterparts, mature DCs (mDCs) inhibit efficient autophagic flux, and block autophagy-mediated lamin degradation upon HSV-1 infection. This in turn prevents HSV-1 nuclear egress and the formation of infectious virions, i.e., H-particles. However, during millions of years of co-evolution, HSV-1 evolved sophisticated strategies to bypass this dead end of replication. Intriguingly, during an HSV-1 infection of mDCs the virus produces non-infectious L-particles (Goldwich et al., 2011; Turan et al., 2019). While L-particles contain tegument proteins and the glycoprotein rich envelope (Szilágyi and Cunningham, 1991; McLauchlan and Rixon, 1992), these particles are characterized by the lack of the capsid and thus the viral genome. Moreover, in contrast to H-particles, L-particles are present in the cisternae of the rough endoplasmic reticulum (Alemañ et al., 2003; Hogue et al., 2016; Heilingloh and Krawczyk, 2017). Despite these prominent differences among H- and L-particles, both HSV-1-derived particle variants share similar maturation steps, especially in human neuronal cells (Granzow et al., 2001; Alemañ et al., 2003; Ibiricu et al., 2013). However, the biological function of HSV-1-derived L-particles during infection is yet not completely understood and thus requires further investigation to gain more insights into their role during HSV-1 replication and propagation. Concerning this, several authors previously proposed that the presence of L-particles can foster the infectivity of HSV-1 (McLauchlan et al., 1992; Dargan and Subak-Sharpe, 1997). Furthermore, mDC-derived L-particles are capable of modulating non-infected bystander mDCs via the transmission of viral proteins (Heilingloh et al., 2015). In particular, the functionally important glycoprotein CD83 is not only downregulated in directly infected but also in non-infected bystander mDCs via L-particles. Given their modulatory capacity, it seems reasonable to assume that L-particles possess a crucial role during HSV-1 infection.

Within the present study, we intended to get closer insights into the composition of L-particles derived from HSV-1-infected BHK21 cells and mDCs using mass spectrometry. We identified 63 viral proteins in mature infectious virions as well as in L-particles from HSV-1-infected BHK21 cells. Moreover, we report mass spectrometric analyses of L-particles derived from HSV-1-infected mDCs, whereby 41 viral proteins have been identified. Quantification of these proteins revealed that L-particles from the two different cell types possess a different protein composition. HSV-1-derived L-particles from BHK21 cells especially exhibit higher amounts of US2, UL31, UL34, and ICP8 compared to H-particles. By contrast, L-particles produced by mDCs upon HSV-1 infection are different to L-particles from BHK21 cells and are characterized by the high abundance of ICP6, ICP4, glycoprotein B (gB) and gD. Concerning the functional role of L-particles, our results suggest that L-particles modify CD83 surface expression during the DC maturation process as well as impair the T cell stimulatory

capacity of mDCs. Due to the plethora of specific viral proteins incorporated into L-particles, we hypothesize that these non-infectious particles produced by HSV-1-infected mDCs have an immunomodulatory effect on DCs.

MATERIALS AND METHODS

Generation of Dendritic Cells

For the generation of human monocyte-derived mature dendritic cells (mDCs) peripheral blood mononuclear cells (PBMCs) were isolated from leukoreduction system chamber (Pfeiffer et al., 2013). Lymphoprep solution was overlaid with the diluted blood (1:5 in PBS supplemented with 10% ACD-A) and centrifuged at $400 \times g$ for 30 min at RT. The distinct intermediate phase was collected and washed three times with ice-cold PBS containing 1 mM EDTA. Subsequently, the PBMC pellet was resuspended in 10 mL of RPMI 1640. PBMCs (approximately 400×10^6) were centrifuged at $300 \times g$ for 5 min, resuspended in 25 mL DC medium (RPMI 1640 supplemented with 1% human Ab serum, 100 U/mL Penicillin, 100 U/mL Streptomycin, 2 mM L-glutamine and 10 mM HEPES) (all Lonza, Switzerland), transferred into T₁₇₅ cell culture flasks and incubated at 37°C and 5% CO₂ for 1 h. Cells were washed three times with pre-warmed RPMI 1640 (Lonza, Switzerland), and the non-adherent fraction was allowed to adhere in DC medium in an additional cell culture flask with subsequent discarding the non-adherent cells as described above. Adherent monocytes were cultivated in 30 mL of DC medium supplemented with 800 U/mL GM-CSF (Miltenyi Biotec, Germany) and 250 U/mL IL-4 (Miltenyi Biotec, Germany). On the fourth day, 5 mL of fresh DC medium supplemented with 400 U/mL GM-CSF and 250 U/mL IL-4 were added to each cell culture flask to generate iDCs. For the generation of mDCs, a maturation cocktail containing GM-CSF (40 U/mL), IL-4 (250 U/mL), IL-1 β (Cell Genix GmbH, Germany; 200 U/mL), IL-6 (Cell Genix GmbH, Germany; 1,000 U/mL), TNF- α (Peprotech, Germany; 10 ng/mL) and PGE2 (Pfizer, Germany; 1 μ g/mL) was added to each cell culture flask on day 5. Two days after induction of maturation mDCs were used for infection experiments. For the generation of L-particles, mDCs were used 1.5 days post maturation.

Cells, Virus Strain and Amplification

HSV-1/17+/CMV-EGFP/UL43, herein designated as HSV-1, was obtained from the laboratory strain HSV-1 17+ via the insertion of a GFP expression cassette controlled by the CMV promoter into the UL43 locus [BioVex, (Coffin et al., 1996, 1998)]. This gene is not essential for HSV-1 replication and its deletion does not affect HSV-1 reactivation and latency (Mikloska et al., 2001). For virus amplification, 90% confluent BHK21 cells in T₁₇₅ cell culture flasks were washed once with PBS and infected in 5 mL of infection medium (RPMI 1640 with 20 mM HEPES) containing a defined amount of HSV-1 virions (MOI of 0.01). The infection was performed on an orbital shaker at RT for 1 h. Subsequently, 20 mL of DMEM [supplemented with 10% FCS, 2 mM L-glutamine, 100 U/mL Penicillin, 100 U/mL Streptomycin and 1% non-essential amino acids (100 \times stock)] were added to

each cell culture flask and cells were incubated at 37°C and 5% CO₂. Three to four days later, supernatants were collected and centrifuged at $2575 \times g$ for 10 min at 4°C. The supernatant was transferred into high speed centrifugation tubes and centrifuged at $39742 \times g$ for 2 h at 4°C. The virus pellet, which was used for further isolation of L- and H-particles, was overlaid with 150 μ L of MNT buffer (virus stock for infection experiments; 30 mM MES, 100 mM NaCl, 20 mM Tris) or 150 μ L of DMEM without phenol red (high glucose, particle isolation) and stored overnight at 4°C. Virus pellets were resuspended, aliquoted in cryo-vials and stored at -80°C . Virus titration was performed as described elsewhere (Grosche et al., 2019). The BHK21 cell line is one of the cell lines generally used for HSV-1 amplification generating both H- and L-particles. In contrast, mDCs established a mechanism to counteract HSV-1 propagation and only releasing L-particles (Turan et al., 2019).

Isolation of HSV-1-Derived Particles

For particles derived from HSV-1-infected BHK21 cells, 15 T₁₇₅ cell culture flasks of 90% confluent BHK21 cells were inoculated and supernatants were harvested to pellet the virus as described above in “Cells, virus strain and amplification.” For the generation of L-particles derived from HSV-1-infected mDCs, 50×10^6 to 130×10^6 mDCs were infected with HSV-1 using an MOI of 1 in a total volume of 15 to 25 mL infection medium. After 1 h of incubation at 37°C and gentle shaking, cells were centrifuged at $303 \times g$ for 5 min and transferred into DC medium adjusting a final cell concentration of 1.25×10^6 mDCs/mL. At 20 hpi, supernatants of HSV-1-infected mDCs were harvested and virus particles were pelleted as described in “Cells, virus strains and amplification.” Since the lifetime of mDCs is limited and the replication cycle is abortive in mDCs, compared to the complete replication cycle in BHK21 cells, the incubation time of mDCs and BHK21 cells is different. H- and/or L-particles were isolated via a first centrifugation of supernatants from HSV-1-infected cells (centrifuged at $39742 \times g$ as described above) according to a previously published protocol (Szilágyi and Cunningham, 1991). In brief, virus suspension was loaded onto a gradient of 5–20% Ficoll PM 400 (Sigma-Aldrich, Deisenhofen, Germany) and centrifuged at $26,000 \times g$ for 2 h at 4°C. Subsequently, H- particles and L-particles were collected by punctation with a needle. Finally, isolated H- and L-particles-containing suspensions were transferred into centrifugation tubes (Beckman Coulter, Brea, United States), filled up with 30 mL DMEM without phenol red and samples were centrifuged at $80,000 \times g$ for 2 h at 4°C. The pellets were resuspended in an appropriate amount of DMEM without phenol red according to the virus pellet size and stored at -80°C until further usage. L-particles were UV-irradiated three times applying 0.12 J/cm² in a Vilber Luormat (Biometra, Göttingen, Germany), in order to inactivate contaminating H-particles.

Electron Microscopy

Electron microscopy was performed as previously described (Heilingloh et al., 2015). Briefly, in a first step, dialysis of H- and L-particle preparations against 20 mM HEPES was performed in a SnakeSkin pleated dialysis tube (10000-molecular-weight

cutoff, Thermo Scientific, Rockford, IL, United States) overnight at 4°C. Afterward, particles were seeded on carbon-coated 400-square-mesh copper grids (Electron Microscopy Sciences, Hatfield, PA, United States) for 20 min at RT and fixed with 2% glutaraldehyde. Finally, particles were stained with 1% uranyl acetate (diluted in 50% ethanol) for 10 min and subsequently with lead citrate for 5 min. For data analysis a transmission electron microscope (Leo 912; Zeiss, Oberkochen, Germany) was used.

Preparation of Particle Lysates and Immunoblotting

An aliquot of isolated H- and L-particle solutions was mixed with 4× Roti-Load 1 (Carl Roth GmbH, Germany; final concentration: 1×) and denatured at 95°C for 10 min. Protein samples were loaded onto 10% SDS polyacrylamide gels (SDS-PAA) and separated using SDS-PAGE. Afterward, proteins were transferred onto a nitrocellulose membrane by wet transfer or SDS-gel was incubated with coomassie staining solution (0.05% Coomassie Brilliant Blue R-250 (BioRad 161-0400), 20% isopropanol, 10% acetic acid) at 50°C for 10 min. Subsequently, gels were washed once in 10% acetic acid at RT for 1h and further destained in ddH₂O overnight at RT. For L-particles derived from mDCs, SDS-gel was stained using the SilverQuest staining Kit (Invitrogen, California, United States) according to manufacturing instructions. In case of Western blotting, the membrane was blocked in 1× Roti-block (Carl Roth GmbH, Germany) for 1 h, and incubated with primary antibodies overnight at 4°C. The antibodies were detected via Image Quant and ECL using Amersham ECL Prime Western blotting detection reagent (GE Healthcare, Solingen, Germany) after the membrane was incubated with a species-specific HRP-conjugated secondary antibody. All used antibodies are listed next: ICP5 antibody (Santa cruz, sc-56989, clone 3B6), gB antibody (Santa cruz, sc-56987, clone 10B7), ICP4 antibody (Santa cruz, sc-56986, clone 10F1), ICP0 antibody (Santa cruz, sc-53070, clone 11060), gD antibody (Santa cruz, sc-21719, clone DL6), ICP8 antibody (Santa cruz, sc-53329, clone 10A3) and UL42 antibody (Santa cruz, sc-53331, clone 13C9) (all primary antibodies were diluted 1:1,000), polyclonal anti-mouse-IgG HRP-linked (Cell signaling, 1:2,500).

Mass Spectrometry Analyses

For mass spectrometric analyses, we used MS1-based label-free quantification. This method is based on the quantification of peptide signals at the MS1 level after tryptic digestion (Pappireddi et al., 2019). The total peak areas of the peptide are integrated over the time. For subsequent relative quantification, the intensities (“sum of the ion peak intensities of unique peptides”) of each peptide in one experiment is compared to the respective signals in other experiments (Bantscheff et al., 2007). The unique peptides in our analysis are those ones which are used for the MS1-based label-free quantification between the samples.

Samples were prepared as follows: L- and H-particle preparations from HSV-1-infected BHK21 cells and mDCs were lysed in 4× Roti-Load 1 (Carl Roth GmbH, Germany; final concentration: 1×) and subsequently denatured at 95°C for 10 min. Samples were processed for MS1-based label-free

quantification by a modified filter-aided sample preparation method (Wiśniewski et al., 2009; Lamm et al., 2017). The 10 kD cutoff filter (Microcon YM-10, Vivacon 500; Sartorius) was washed once with 8 M Urea supplemented with 50 mM Tris (pH 8.0; washing buffer). After each loading or washing step, the filter was centrifuged at 12.000 × g until dryness. Approximately 3.5 μg (mDC particles) or 20 μg (BHK21 particles) of sample preparation was mixed with 200 μL washing buffer and a maximum of 300 μL of the sample solution was loaded onto the filter unit. If the sample volume exceeded the maximal volume, sample loading was repeated until the entire sample was loaded. The filter unit was washed three times with washing buffer. Subsequently, samples were reduced using 25 mM DTT in washing buffer at 37°C for 30 min at 600 rpm. Afterward, samples were alkylated with 25 mM chloroacetamide present in the washing buffer at RT for 30 min in the dark. Filter units were washed with washing buffer until foam formation in the flow through disappeared. Protein-loaded filter units were washed with 6 M Urea supplemented with 50 mM Tris (buffer B) and afterward incubated with buffer B supplemented with 50 μL of 0.5 μg Lys-C (Wako Chemicals) at 37°C for 3h at 600 rpm. Subsequently, a final concentration of 1 M urea was adjusted using 50 mM Tris buffer (= dilution buffer) and protein samples were trypsinized using 1 μg trypsin at 37°C and 600 rpm overnight. The filter units were washed with 100 μL washing buffer and the flow through was collected in low binding tubes after centrifugation. The peptides were acidified up to a final concentration of 0.5% TFA. Subsequently, peptide samples were desalted using C18 membrane stage tips, which were activated using 100% acetonitrile (ACN). After a 2 min centrifugation step at 800 × g, peptide samples were loaded onto the columns. The columns were washed with 1% ACN supplemented with 0.1% TFA and a defined amount of peptides was eluted into fresh 1.5 mL low binding tubes, using 50% ACN containing 0.1% TFA. Afterward, peptides were vacuum concentrated and resuspended in 1% ACN supplemented with 0.1% TFA. All peptide samples were separated by reverse phase chromatography with a linear increase of acetonitrile on a nano flow Ultimated 3000 HPLC (Dionex) with a flow rate of 200 nL/min. Separated peptides were ionized by an EASY-Spray ion source (Thermo Fisher Scientific) with 2.0 kV and 275°C of the transfer capillary. All samples were analyzed by an Orbitrap Fusion tribrid (Thermo Scientific) working in a positive polarity mode. Detailed mass spectrometry scan settings were previously described (Kraner et al., 2017). Raw data were analyzed using PEAKS Studio 8.5 [Bioinformatics Solutions, Waterloo, Ontario, Canada; (Zhang et al., 2012)] against a combined host-viral database using the HHV1 uniprot.org database [downloaded in November 2018 (BHK21 cell-derived particles) and July 2019 (mDC-derived particles)], *Homo sapiens* uniprot.org database (downloaded in July 2019, mDC-derived particles) or *Mesocricetus auratus* uniprot.org database (downloaded in May 2020, BHK21 cell-derived particles). Oxidation of methionine and carbamidomethylation of cysteines were set as dynamic and static modifications, respectively. Proteins included into data interpretation must exhibit a false discovery rate of <1%. For evaluation of the

data we normalized the intensity of each protein to the mean of all glycoproteins detected in three mDC or four BHK21 particle preparations. The analyzed data sets represent three or four replicates for mDC- or BHK21 cell-derived HSV-1 particles, respectively.

Infection of iDCs and Flow Cytometric Analyses of the Maturation Phenotype

To analyze DC activation phenotype prior and post incubation with HSV-1 virions or HSV-1-derived L-particles, 0.6×10^6 cells were mock- or HSV-1-infected (MOI of 2) or treated with UV-inactivated HSV-1 (viral material corresponding to MOI of 20, $8 \times 0.12 \text{ J/cm}^2$) or HSV-1 L-particles (viral material corresponding to high MOI, $3 \times 0.12 \text{ J/cm}^2$). The infection was performed in 300 μL infection medium supplemented with the defined amount of HSV-1-derived virions or L-particles. At 1 hpi, iDCs including the infection medium were transferred directly into DC medium containing the maturation cocktail as described in “Generation of dendritic cells” in a final concentration of 1×10^6 cells/mL. Cells were harvested 24 hpi and prepared for flow cytometric analyses. In brief, cells were washed once with FACS buffer (PBS containing 2% FCS) and incubated with LIVE/DEAD Fixable Violet dead cell stain (Life Technologies, Carlsbad, CA, United States) and specific antibodies against mouse anti-human CD11c (BD Bioscience, PE-Cy5, clone: B-ly6), mouse anti-human CD83 (Invitrogen, APC, clone: HB15e), mouse anti-human CD80 (BD Pharmingen, PE, clone: L307.4), rat anti-human CCR7 (CD197) (BD Pharmingen, PE-Cy7, clone: 3D12), anti-human HLA-DR (Bio Legend, APC/Cy7, clone: L243) at 4°C for 30 min in the dark. Finally, cells were washed two times with FACS buffer, fixed with 2% PFA in FACS buffer and measured using FACS Canto II flow cytometer (BD) and analyzed with FCS express five flow research edition software.

Mixed Lymphocyte Reaction (MLR)

Mature DCs were infected with purified H-particles (MOI of 2), incubated with UV-inactivated H-particles ($8 \times 0.12 \text{ J/cm}^2$, viral material corresponding to MOI of 20) or purified L-particles (viral material corresponding to high MOI, $3 \times 0.12 \text{ J/cm}^2$) or left untreated (mock control). At 8 hpi, cells were harvested and titrated numbers of mDCs were cocultured with 0.4×10^6 allogeneic T cells derived from the non-adherent fraction of PMBCs (Pfeiffer et al., 2013). After additional 72 h of incubation in a 96-well flat bottom plate, cocultures were pulsed with 1 $\mu\text{Ci/well}$ [^3H]-thymidine (PerkinElmer) for 16 h before they were harvested onto glassfiber filtermates using an ICH-110 harvester (Inotech). Counts per minutes were measured in a 1450 microplate counter (Wallac). For the evaluation of the MLR, the mean of the duplicates for each condition was calculated.

Statistical Analyses

Results of mass spectrometric analyses are displayed as individual intensity per replicate or mean intensity of all replicates as stated in the respective figure legend. Data regarding DC maturation phenotype or MLR are shown as median or counts per minutes \pm standard error of the mean (SEM) as indicated.

For the determination of the significance, data were analyzed using one-way analysis of variance (ANOVA) and Bonferroni's multiple-comparison *post hoc* test. Significance was accepted for *p*-values less than 0.05. ****; indicates $p \leq 0.0001$; *** $p \leq 0.001$; ** $p \leq 0.01$; * $p \leq 0.05$; and ns, not significant.

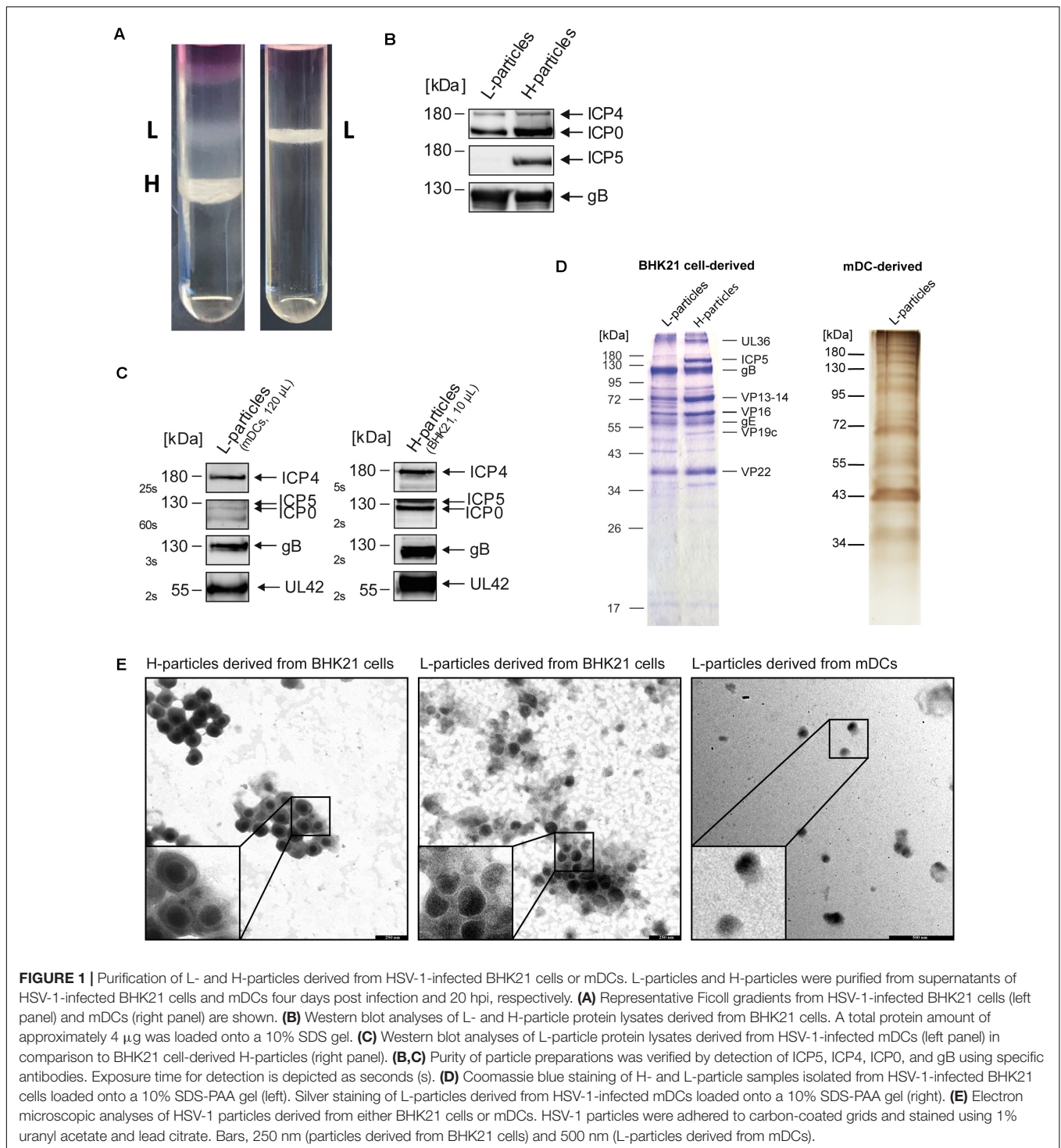
Approvals and Legal Requirements

The local ethics committee has given the permission to generate monocyte-derived DCs from leukapheresis products of healthy donors (reference number: 184_16Bc). This study was carried out in accordance with the recommendations of the ethics committee of the “Friedrich-Alexander-Universität Erlangen-Nürnberg,” with written informed consent from all subjects. All subjects gave written informed consent in accordance with the Declaration of Helsinki.

RESULTS

Distinct Viral Protein Distribution Among BHK21 Cell- and mDC-Derived HSV-1 L-Particles

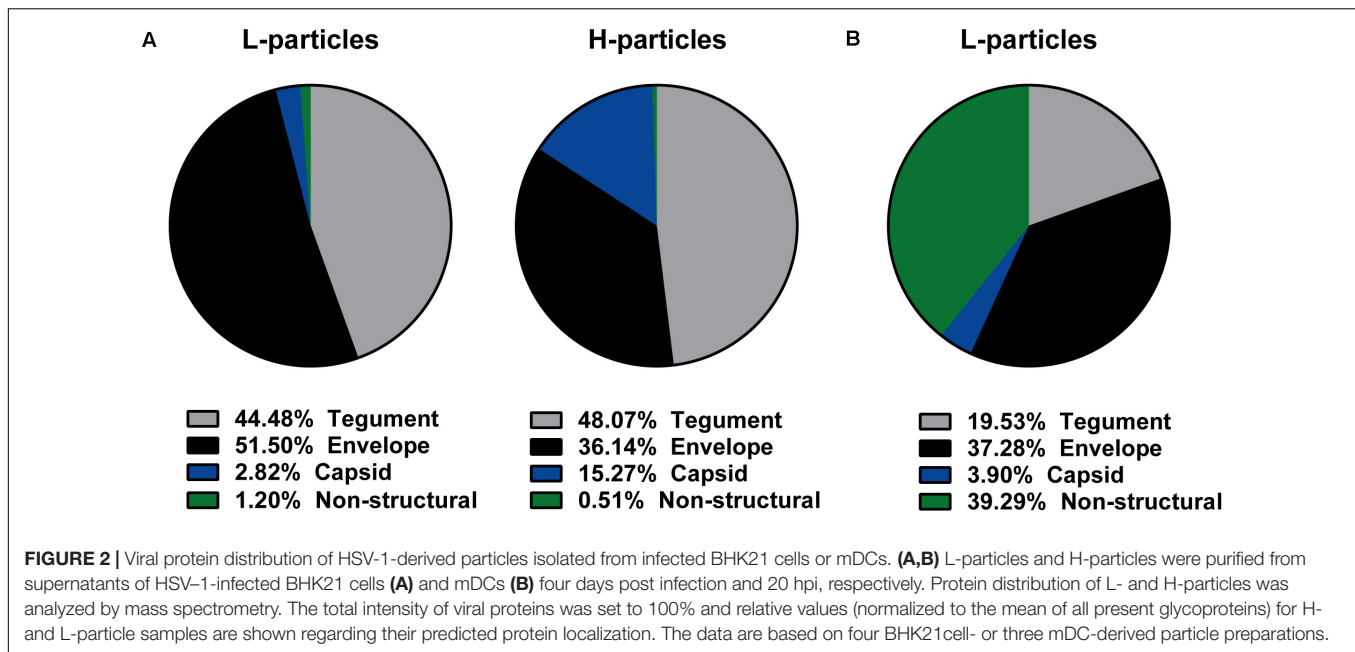
In a comparative analysis, the protein composition of L- and H-particles from HSV-1-infected BHK21 cells and L-particles from HSV-1-infected mDCs was examined using MS1-based label-free quantification. For this, BHK21 cells and mDCs were infected with HSV-1 and supernatants of infected cells were harvested after four days and 20 h post infection (hpi), respectively. The difference in the incubation time is due to the limited life time of DCs and the abortive replication cycle in mDCs compared to complete replication in BHK21 cells. Subsequently, L- and H-particles were isolated using a Ficoll gradient followed by ultracentrifugation. As expected, HSV-1-infected BHK21 cells release both H- and L-particles (**Figure 1A**, left panel). As recently reported, the release of H-particles by HSV-1-infected mDCs is limited due to the block of nuclear egress by the inhibition of autophagic flux upon DC maturation (Turan et al., 2019). **Figure 1A** (right panel) confirms this observation, since the supernatants of HSV-1-infected mDCs almost exclusively contained L-particles and only barely detectable amounts of H-particles. Prior to mass spectrometric analyses, a potential H-particle contamination in the L-particle preparations was verified by the absence of major capsid protein ICP5 in L-particle protein lysates (**Figure 1B**). Moreover, the detection of ICP4, ICP0, gB, and UL42 confirmed the successful isolation of sufficient amounts of either L-particles (mDCs) or H-particles (BHK21 cells; **Figure 1C**). Apart from Western blot detection, the overall protein distribution in L- and H-particles preparations from HSV-1-infected BHK21 cells and mDCs was analyzed via coomassie blue and silver staining of the SDS-PAA gels, respectively (**Figure 1D**). Based on this, a distinct viral protein pattern of both particle variants as well as the exclusive presence of ICP5 and VP19c in H-particles was observed. Regarding the molecular weight of selected viral proteins, the most likely candidates are indicated and revealed the lower abundance of VP13-14 (UL47) in L-particles compared



to H-particles (**Figure 1D**). To verify the purity of L- and H-particle fractions, we analyzed the preparations via electron microscopy (**Figure 1E**). The fraction of the BHK21-derived H-particles showed the characteristic nucleocapsid (black circles within virions) surrounded by the viral envelope. In contrast, the HSV-1 L-particle fractions derived from BHK21 cells and mDCs were more heterogeneous in size, compared to full virions, and

are lacking the viral capsid. The here presented data clearly show that we used pure particle preparations.

Subsequently, MS1-based label-free quantification was performed to decipher these differences in the protein pattern. We used four independent L- and H-particle preparations from HSV-1-infected BHK21 cells and three L-particle preparations isolated from HSV-1-infected mDCs. **Figure 2** shows the



schematic distribution of all detected viral proteins regarding their predicted localization in HSV-1 particles from BHK21 cells (**Figure 2A**) or mDCs (**Figure 2B**). H- and L-particles derived from HSV-1-infected BHK21 cells comprised 63 viral proteins, while L-particle samples from mDCs contained 41 viral proteins. The mean intensity of each viral protein of all samples was calculated and all viral proteins were sorted regarding their predicted localization. Finally, the total intensities of tegument, envelope, capsid and non-structural proteins were set relative to the total intensity of all detected proteins.

Since L-particles are characterized by the lack of the viral capsid, only ~3% (BHK21 cells) to ~4% (mDCs) of the overall protein quantity were capsid-associated proteins, whereas this percentage was five-fold higher in H-particle preparations from BHK21 cells (**Figures 2A,B**). Moreover, the marginal incorporation of capsid proteins in L-particles derived from HSV-1-infected BHK21 cells seemed to be substituted by envelope proteins, since half of all viral L-particle proteins (51.50%), but only one third (36.14%) of all viral H-particle proteins, were found within envelope proteins. In contrast, the percentage of tegument proteins was unaltered between both particle types isolated from BHK21 cells (44–48%). Thus, our mass spectrometric data reveal a shift regarding the percentage of the viral protein distribution in L-particle compared to H-particle preparations derived from HSV-1-infected BHK21 cells, i.e., from capsid toward envelope proteins. L-particles derived from HSV-1-infected mDCs showed a different overall protein distribution, characterized by the extremely high abundance of viral proteins annotated as non-structural proteins, compared to BHK21 cell-derived L-particles (**Figures 2A,B**). Approximately three quarters of all detected viral proteins in L-particles from HSV-1-infected mDCs were associated with the envelope (37.28%) or were categorized as non-structural proteins (39.29%), whereas only ~20% of the viral proteins were localized in the tegument.

Taken these results, L-particles derived from HSV-1-infected mDCs seem to abundantly incorporate distinct viral proteins, i.e., annotated as non-structural proteins, compared to those derived from BHK21 cells.

Highly Sensitive Mass Spectrometric Analysis Reveals 63 and 41 Viral Proteins in Viral Particle Preparations of HSV-1-Infected BHK21 Cells and mDCs, Respectively

Apart from comparing the overall protein distribution in L- versus H-particles derived from different HSV-1-infected cell types, changes in the viral protein pattern were analyzed for each identified viral protein individually. The following tables summarize all detected viral proteins in H- and L-particle preparations according to their localization in either of the particle types (**Tables 1, 2**). Moreover, the detection coverage as well as the number of unique peptides is depicted. In the last decades, the composition of L-particles has been barely investigated, recently only one research group analyzed viral proteins incorporated into L-particles and H-particles in a mass spectrometry-based attempt (Russell et al., 2018). In particular, Russell et al. (2018) identified 51 and 42 viral proteins in preparations of H- and L-particles, respectively, derived from HSV-1 strain Sc16-infected HaCaT cells. Our mass spectrometric data extend this previous report based on the identification of 63 viral proteins in both L- and H-particle samples from HSV-1 strain 17-infected BHK21 cells. Among viral proteins in particles derived from BHK21 cells we identified 24 tegument proteins, 16 proteins belonging to the envelope and eight were annotated as capsid proteins. The remaining 15 viral proteins were designated as non-structural proteins. Furthermore, we affirmed the incorporation

of all recently discovered tegument and glycoproteins which have been identified in previous publications (Loret et al., 2008; Loret and Lippé, 2012; Russell et al., 2018). Concerning ICP34.5, which represents one notable exception, our HSV-1 particle preparations are in line with those reported by Russell et al. (2018), also documenting the absence of this viral protein, whereas previously published mass spectrometric analyses reported the presumed presence of this viral protein based on the detection of a single unique peptide (Loret et al., 2008). Beyond this, our data confirmed the presence of UL20, UL34 and the glycoproteins gK and gN and we successfully identified all five IE proteins, i.e., ICP0, ICP4, ICP22, ICP27, ICP47 and DNA-associated proteins, such as ICP8, UL5, UL30, UL42, and UL52.

More importantly, 41 viral proteins were also detected in L-particles released by HSV-1-infected mDCs. We identified 16 proteins annotated as tegument proteins, nine as envelope proteins, six as capsid proteins and 10 viral proteins as non-structural proteins. Our data of MS1-based label-free quantification further demonstrate that L-particles released by HSV-1-infected mDCs contained only three out of five viral IE proteins (ICP0, ICP4, and ICP27) and high amounts of the glycoproteins gB and gD. As already observed in the overall protein distribution (Figure 2), the intensity of non-structural proteins is notably higher in mDC-derived, compared to BHK21 cell-derived, HSV-1 L-particles (Tables 1, 2).

L-Particles From HSV-1-Infected BHK21 Cells Contain H-Particle-Associated Proteins at Different Quantities

Decoding the protein pattern of L-particles is essential to get deeper insights into the biological role of these non-infectious particles during an HSV-1 infection. Our mass spectrometry-based data revealed 63 viral proteins to be incorporated into HSV-1-derived H- and L-particles produced by infected BHK21 cells. The intensity of these detected viral proteins was normalized to the respective mean intensity of all glycoproteins detected in the respective sample preparation. Subsequently, the ratio of L- versus H-particles was determined for each normalized value (Figure 3). However, a higher ratio of a protein in L-particles does not equate a higher abundance in absolute amounts.

The envelope represents the glycoprotein-rich outer membrane of herpesvirus particles. As shown in Figure 2A, L-particles contained higher levels of specific envelope proteins than H-particles (Figure 3A). Exclusively two proteins of this group, i.e., UL34 and gB, were significantly overrepresented in L-particles. In sharp contrast, gC, gL, gH, gM, US9, and gN were detected at lower amounts in L-particles compared to H-particles, however, gL, gH, and gM were still present in L-particles (see values beside Figure 3A). Interestingly, two third of tegument proteins were underrepresented in L-particles, compared to H-particles (Figure 3B, ratio <1). In contrast, our data revealed that the tegument proteins US2, UL31, UL50, ICP0, and US3 were more abundant in L-particles compared to their infectious counterparts (~1.4 to 2.2-fold). Two proteins, namely ICP4 and the viral thymidine kinase (UL23), were almost similarly

integrated into both particle types (ratio ~1). As expected, the here presented data of MS1-based label-free quantification confirmed that capsid related proteins were significantly underrepresented in L-particles from HSV-1-infected BHK21 cells compared to H-particle preparations, indicating a high purity of these L-particle preparations (Figure 3C). One notable exception was UL6, the portal forming protein for entry of viral DNA into the capsid, which was found to be equally distributed among L- and H-particles from BHK21 cells (Newcomb et al., 2001; Trus et al., 2004). Moreover, our data clearly showed that the capsid proteins UL17 and UL25, promoting the insertion and retention of viral DNA, were present in H-particle samples as already described to be incorporated into HSV-1 virions (McNab et al., 1998; Salmon et al., 1998; Toropova et al., 2011). Furthermore, regarding the L-particle composition, our mass spectrometric data are in line with previous reports showing that the two capsid proteins UL17 and UL6 are present in L-particles (Thurlow et al., 2005). Our results show that the major capsid protein, ICP5, was more abundant in H-particles compared to L-particles, resulting in the lowest L- to H-particle ratio regarding capsid proteins. However, we cannot exclude the possibility of small H-particle contaminations in our L-particle preparations. The remaining non-structural proteins mainly include proteins that were overrepresented in L-particles. For example, ICP8, the major DNA binding protein, is one of the strongest differentially incorporated protein in L-particles compared to H-particles, revealing a 10-fold higher abundance in L-particles (Figure 3D). However, it has to be pointed out that the overall intensity of these non-structural proteins is very low in general and thus the comparison of non-structural proteins in BHK21 cell-derived HSV-1 particles should be treated with caution. In conclusion, our data demonstrate the presence of 63 viral proteins in H- and L-particles which are integrated to distinct extents into either of both particle types derived from infected BHK21 cells.

HSV-1 L-Particles Derived From Infected mDCs Contain High Amounts of gB, gD, ICP6, ICP4, and UL23

Our mass spectrometry-based data revealed 41 viral proteins to be incorporated into L-particles produced by HSV-1-infected mDCs. Figure 4 illustrates the individual intensities of all detected viral proteins, normalized to the mean intensity of all glycoproteins, in the three mDC L-particle replicates, depicted as bar graphs or heat maps. The most abundant viral proteins were associated with the envelope or non-structural proteins. As already shown by our initial Western blot analyses, L-particles from mDCs contained high amounts of ICP4, gB and UL42 (Figure 1C). These observations, including the low presence of ICP0 in L-particles and the high abundance of gB and gD as major envelope proteins, were confirmed by our mass spectrometric results (Figures 4A–C). Again, capsid-associated viral proteins were barely detectable in our L-particle samples from HSV-1-infected mDCs, which confirms the lack of viral capsids in these preparations (Figure 4D). Since HSV-1-infected mDCs

TABLE 1 | Mass spectrometric identification of viral proteins in L-particles derived from HSV-1-infected mDCs.

mDC-derived L-particles										
	Accession	Protein name	Gene name	Coverage (%)	#Unique peptides for quantification	Mean intensity		MW	Description	
Tegument	P08393 ICP0_HHV11	ICP0	RL2	3	1	2.03E-02		78457	E3 ubiquitin-protein ligase ICP0	
	P08392 ICP4_HHV11	ICP4	RS1	25	19	5.54E-01	█	132844	Major viral transcription factor ICP4	
	P10221 ITP_HHV11	ICP32	UL37	32	26	3.69E-01	█	120556	Inner tegument protein	
	P10191 CEP1_HHV11	UL7	UL7	20	4	5.24E-02		33059	Cytoplasmic envelopment protein 1	
	P04290 UL13_HHV11	UL13	UL13	10	3	4.56E-02		57197	Serine/threonine-protein kinase UL13	
	P04291 TEG3_HHV11	UL14	UL14	21	2	4.73E-02		23934	Tegument protein UL14	#
	P10205 TEG4_HHV11	UL21	UL21	2	1	3.49E-02		57642	Tegument protein UL21	#
	P03176 KITH_HHV11	UL23	UL23	31	8	7.30E-01	█	40972	Thymidine kinase	
	P10235 TEG7_HHV11	UL51	UL51	16	3	1.75E-01	█	25470	Tegument protein UL51	
	P06485 US02_HHV11	US2	US2	29	6	1.52E-01	█	32471	Protein US2	
	P04413 US03_HHV11	US3	US3	7	2	2.67E-02		52835	Serine/threonine-protein kinase US3	#
	P10225 SHUT_HHV11	vhs	UL41	5	2	2.06E-02		54918	Virion host shutoff protein	#
	P10230 TEG1_HHV11	VP11-12	UL46	21	10	2.96E-01	█	78241	Tegument protein UL46	
	P10231 TEG5_HHV11	VP13-14	UL47	8	3	5.45E-02		73817	Tegument protein UL47	#
	P06492 VP16_HHV11	VP16	UL48	20	6	1.32E-01	█	54345	Tegument protein VP16	
P10233 VP22_HHV11	VP22	UL49	38	8	2.25E-01	█	32254	Tegument protein VP22		
Envelope	P10211 GB_HHV11	gB	UL27	28	19	2.23E+00	█	100292	Envelope glycoprotein B	
	Q69091 GD_HHV11	gD	US6	43	12	1.91E+00	█	43347	Envelope glycoprotein D	
	P04488 GE_HHV11	gE	US8	17	6	2.59E-01	█	59094	Envelope glycoprotein E	
	P06477 GH_HHV11	gH	UL22	27	14	4.58E-01	█	90366	Envelope glycoprotein H	

(Continued)

TABLE 1 | Continued

mDC-derived L-particles										
	Accession	Protein name	Gene name	Coverage (%)	#Unique peptides for quantification	Mean intensity		MW	Description	
	P68331 GK_HHV11	gK	UL53	4	1	4.01E-02		37573	Envelope glycoprotein K	#
	P10185 GL_HHV11	gL	UL1	15	2	1.47E-01	■	24934	Envelope glycoprotein L	
	P10218 NEC2_HHV11	UL34	UL34	32	5	1.16E-01	■	29790	Nuclear egress protein 2	
	P10229 EV45_HHV11	UL45	UL45	18	2	6.00E-02		18180	Envelope protein UL45	
	P10240 UL56_HHV11	UL56	UL56	36	5	3.90E-01	■	21184	Protein UL56	
Capsid	P06491 MCP_HHV11	ICP5	UL19	32	29	2.38E-01	■	149083	Major capsid protein	
	P10201 CVC1_HHV11	UL17	UL17	7	3	8.75E-02		74582	Capsid vertex component 1	
	P10209 CVC2_HHV11	UL25	UL25	10	4	3.74E-02		62670	Capsid vertex component 2	
	P32888 TRX1_HHV11	VP19c	VP19c	4	1	4.20E-03		50263	Triplex capsid protein 1	#
	P10202 TRX2_HHV11	UL18	UL18	41	7	2.00E-01	■	34271	Triplex capsid protein 2	
	P10210 SCAF_HHV11	VP24	UL26	6	2	1.88E-02		66471	Capsid scaffolding protein	
Non-structural	P08543 RIR1_HHV11	ICP6	UL39	52	46	3.40E+00	■	124050	Ribonucleoside-diphosphate reductase large subunit	
	P04296 DNBI_HHV11	ICP8	UL29	34	24	7.40E-01	■	128350	Major DNA-binding protein	
	P10224 RIR2_HHV11	ICP10	UL40	31	7	3.34E-01	■	38019	Ribonucleoside-diphosphate reductase small subunit	
	P10238 ICP27_HHV11	ICP27	UL54	3	1	5.38E-02		55253	mRNA export factor	
	P10186 UNG_HHV11	UL2	UL2	11	3	5.56E-01	■	36328	Uracil-DNA glycosylase	
	P10189 HELI_HHV11	UL5	UL5	5	3	1.04E-02		98715	DNA replication helicase	
	P04294 AN_HHV11	UL12	UL12	21	10	5.82E-01	■	67508	Alkaline nuclease	
	P10208 UL24_HHV11	UL24	UL24	6	1	1.13E-02		29476	Protein UL24	#
	P10216 UL32_HHV11	UL32	UL32	3	1	5.82E-03		63950	Packaging protein UL32	#
	P10226 PAP_HHV11	UL42	UL42	27	8	2.10E-01	■	51159	DNA polymerase processivity factor	

































L-particles were purified from supernatants of HSV-1-infected mDCs cells using a Ficoll gradient. Subsequently, samples were prepared for mass spectrometric analyses. Proteins are summarized regarding their predicted localization in the viral particle in numerical order and mean intensities of all three replicates are normalized to mean of all glycoproteins detected in at least two out of three samples. "MW" means molecular weight. Proteins detected in two out of three samples are marked with "#."

TABLE 2 | Mass spectrometric identification of viral proteins in H-particles and L-particles derived from HSV-1-infected BHK21 cells.

BHK21-derived H- and L-particles												
	Accession	Protein name	Gene name	Coverage (%)	#Unique peptides for quantification	Mean L intensity		Mean H intensity		MW	Description	Previously identified
Tegument	P08393	ICP0	RL2	69	102	6.36E-01	■	4.62E-01	■	78457	E3 ubiquitin-protein ligase ICP0	Y
	ICP0_HHV11											
	P08392	ICP4	RS1	81	106	2.41E-01	■	2.28E-01	■	132844	Major viral transcription factor ICP4	Y
	ICP4_HHV11											
	P10221	ICP32	UL37	77	98	1.40E-01	■	6.56E-01	■	120556	Inner tegument protein	Y
	ITP_HHV11											
	P10191	UL7	UL7	49	12	3.67E-02		4.62E-02		33059	Cytoplasmic envelopment protein 1	Y
	CEP1_HHV11											
	P04289	UL11	UL11	61	4	1.87E-02		2.55E-02		10487	Cytoplasmic envelopment protein 3	Y
	CEP3_HHV11											
	P04290	UL13	UL13	60	26	1.16E-01	■	1.56E-01	■	57197	Serine/threonine-protein kinase UL13	Y
	UL13_HHV11											
	P04291	UL14	UL14	33	6	3.31E-02		4.42E-02		23934	Tegument protein UL14	Y
	TEG3_HHV11											
	P10200	UL16	UL16	87	28	1.77E-01	■	3.78E-01	■	40443	Cytoplasmic envelopment protein 2	Y
	CEP2_HHV11											
	P10205	UL21	UL21	76	56	5.10E-01	■	7.05E-01	■	57642	Tegument protein UL21	Y
	TEG4_HHV11											
	P03176	UL23	UL23	36	13	2.91E-02		2.88E-02		40972	Thymidine kinase	Y
	KITH_HHV11											
P10215	UL31	UL31	23	7	8.62E-03		4.15E-03		33953	Nuclear egress protein 1	Y	
NEC1_HHV11												
P10220	UL36	UL36	70	252	3.05E-01	■	9.92E-01	■	335863	Large tegument protein deneddylase	Y	
LTP_HHV11												
P10234	UL50	UL50	53	14	1.99E-02		1.22E-02		39128	Deoxyuridine 5'-triphosphate nucleotidohydrolase	Y	
DUT_HHV11												
P10235	UL51	UL51	64	12	5.53E-02		9.17E-02	■	25470	Tegument protein UL51	Y	
TEG7_HHV11												
P10239	UL55	UL55	36	4	8.21E-03		9.27E-03		20493	Tegument protein UL55	Y	
TEG6_HHV11												

(Continued)

TABLE 2 | Continued

BHK21-derived H- and L-particles										
Accession	Protein name	Gene name	Coverage (%)	#Unique peptides for quantification	Mean L intensity	Mean H intensity	MW	Description	Previously identified	
P06485 US02_HHV11	US2	US2	87	32	1.75E-01 	8.27E-02 	32471	Protein US2	Y	
P04413 US03_HHV11	US3	US3	58	29	1.70E-01 	1.24E-01 	52835	Serine/threonine-protein kinase US3	Y	
P06486 US10_HHV11	US10	US10	48	17	8.79E-02 	1.53E-01 	34056	Virion protein US10	Y	
P04487 RNB_HHV11	US11	US11	40	6	8.04E-02 	6.78E-02 	17757	RNA-binding protein	Y	
P10225 SHUT_HHV11	vhs	UL41	61	34	1.16E-01 	2.65E-01 	54918	Virion host shutoff protein	Y	
P10230 TEG1_HHV11	VP11-12	UL46	78	107	6.25E-01 	7.38E-01 	78241	Tegument protein UL46	Y	
P10231 TEG5_HHV11	VP13-14	UL47	83	139	2.06E+00 	3.43E+00 	73817	Tegument protein UL47	Y	
P06492 VP16_HHV11	VP16	UL48	74	79	1.51E+00 	2.74E+00 	54345	Tegument protein VP16	Y	
P10233 VP22_HHV11	VP22	UL49	83	72	3.31E+00 	4.89E+00 	32254	Tegument protein VP22	Y	
Envelope P10211 GB_HHV11	gB	UL27	71	158	4.66E+00 	2.58E+00 	100292	Envelope glycoprotein B	Y	
P10228 GC_HHV11	gC	UL44	13	4	4.11E-03 	5.84E-03 	54998	Envelope glycoprotein C	Y	
Q69091 GD_HHV11	gD	US6	63	58	2.31E+00 	2.79E+00 	43347	Envelope glycoprotein D	Y	
P04488 GE_HHV11	gE	US8	64	82	1.60E+00 	1.75E+00 	59094	Envelope glycoprotein E	Y	
P06484 GG_HHV11	gG	US4	28	7	8.27E-01 	7.29E-01 	25239	Envelope glycoprotein G	Y	
P06477 GH_HHV11	gH	UL22	55	62	2.68E-01 	4.54E-01 	90366	Envelope glycoprotein H	Y	
P06487 GI_HHV11	gI	US7	39	18	3.67E-01 	3.69E-01 	41370	Envelope glycoprotein I	Y	

(Continued)

TABLE 2 | Continued

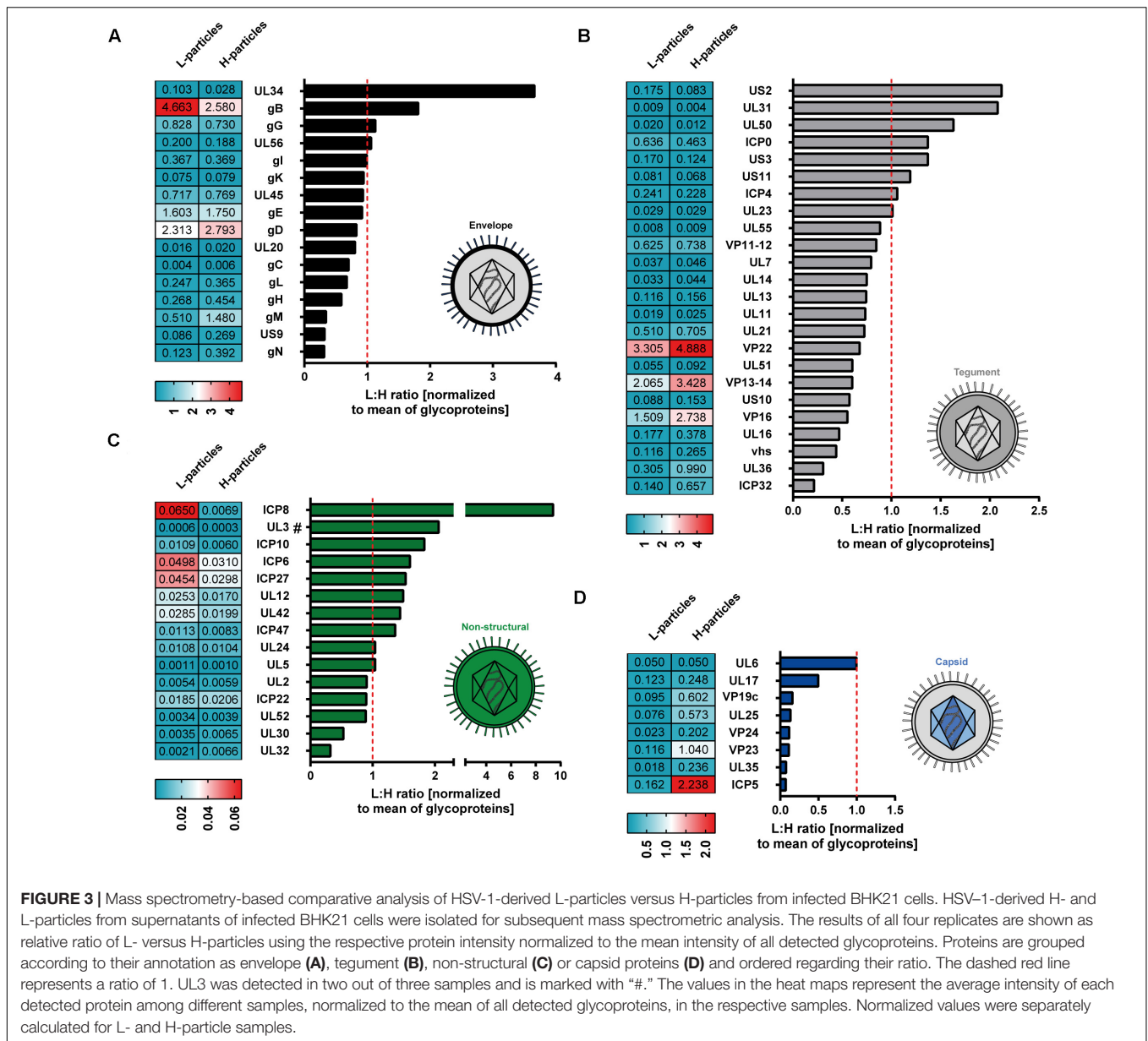
BHK21-derived H- and L-particles											
Accession	Protein name	Gene name	Coverage (%)	#Unique peptides for quantification	Mean L intensity	Mean H intensity	MW	Description	Previously identified		
P68331 GK_HHV11	gK	UL53	28	8	7.47E-02	7.94E-02	37573	Envelope glycoprotein K	Y		
P10185 GL_HHV11	gL	UL1	47	12	2.47E-01	3.65E-01	24934	Envelope glycoprotein L	Y		
P04288 GM_HHV11	gM	UL10	34	28	5.10E-01	1.48E+00	51393	Envelope glycoprotein M	Y		
O09800 GN_HHV11	gN	UL49.5	25	5	1.23E-01	3.92E-01	9202	Envelope glycoprotein N	N		
P10204 UL20_HHV11	UL20	UL20	20	6	1.64E-02	2.04E-02	24231	Protein UL20	Y		
P10218 NEC2_HHV11	UL34	UL34	75	15	1.03E-01	2.81E-02	29790	Nuclear egress protein 2	Y		
P10229 EV45_HHV11	UL45	UL45	73	25	7.17E-01	7.69E-01	18180	Envelope protein UL45	Y		
P10240 UL56_HHV11	UL56	UL56	73	16	2.00E-01	1.88E-01	21184	Protein UL56	Y		
P06481 US9_HHV11	US9	US9	38	15	8.63E-02	2.69E-01	10027	Envelope protein US9	Y		
P06491 MCP_HHV11	ICP5	UL19	76	196	1.62E-01	2.24E+00	149083	Major capsid protein	Y		
P10190 PORTL_HHV11	UL6	UL6	34	25	4.98E-02	5.00E-02	74092	Portal protein	Y		
P10201 CVC1_HHV11	UL17	UL17	77	51	1.23E-01	2.47E-01	74582	Capsid vertex component 1	Y		
P10209 CVC2_HHV11	UL25	UL25	78	45	7.61E-02	5.72E-01	62670	Capsid vertex component 2	Y		
P32888 TRX1_HHV11	VP19c	VP19c	76	39	9.55E-02	6.02E-01	50263	Triplex capsid protein 1	Y		
P10202 TRX2_HHV11	VP23	UL18	79	40	1.16E-01	1.04E+00	34271	Triplex capsid protein 2	Y		
P10210 SCAF_HHV11	VP24	UL26	54	35	2.32E-02	2.02E-01	66471	Capsid scaffolding protein	Y		
P10219 SCP_HHV11	UL35	UL35	91	13	1.78E-02	2.36E-01	12096	Small capsomere-interacting protein	Y		

(Continued)

TABLE 2 | Continued

BHK21-derived H- and L-particles												
	Accession	Protein name	Gene name	Coverage (%)	#Unique peptides for quantification	Mean L intensity		Mean H intensity		MW	Description	Previously identified
Non-structural	P08543	ICP6	UL39	57	48	4.97E-02		3.10E-02		124050	Ribonucleoside-diphosphate reductase large subunit	Y
	RIR1_HHV11											
	P04296	ICP8	UL29	56	55	6.50E-02		6.91E-03		128350	Major DNA-binding protein	N
	DNBI_HHV11											
	P10224	ICP10	UL40	42	12	1.09E-02		5.98E-03		38019	Ribonucleoside-diphosphate reductase small subunit	Y
	RIR2_HHV11											
	P04485	ICP22	US1	24	11	1.84E-02		2.06E-02		46525	Transcriptional regulator ICP22	Y
	ICP22_HHV11											
	P10238	ICP27	UL54	50	23	4.54E-02		2.97E-02		55253	mRNA export factor	Y
	ICP27_HHV11											
	P03170	ICP47	US12	65	5	1.13E-02		8.31E-03		9793	ICP47 protein	N
	ICP47_HHV11											
	P10186	UL2	UL2	27	5	5.35E-03		5.92E-03		36328	Uracil-DNA glycosylase	Y
	UNG_HHV11											
	P10187	UL3	UL3	7	1	6.17E-04		3.00E-04		25609	Nuclear phosphoprotein UL3	N (#)
	NP03_HHV11											
	P10189	UL5	UL5	11	6	1.06E-03		1.02E-03		98715	DNA replication helicase	N
	HELI_HHV11											
	P04294	UL12	UL12	45	23	2.53E-02		1.70E-02		67508	Alkaline nuclease	N
AN_HHV11												
P10208	UL24	UL24	29	7	1.08E-02		1.04E-02		29476	Protein UL24	N	
UL24_HHV11												
P04293	UL30	UL30	12	10	3.44E-03		6.50E-03		136421	DNA polymerase catalytic subunit	N	
DPOL_HHV11												
P10216	UL32	UL32	9	5	2.12E-03		6.62E-03		63950	Packaging protein UL32	N	
UL32_HHV11												
P10226	UL42	UL42	55	21	2.85E-02		1.98E-02		51159	DNA polymerase processivity factor	N	
PAP_HHV11												
P10236	UL52	UL52	10	7	3.45E-03		3.89E-03		114423	DNA primase	N	
PRIM_HHV11												

L-particles and H-particles were purified from supernatants of HSV-1-infected BHK21 cells using a Ficoll gradient. Subsequently, samples were prepared for mass spectrometric analyses. Proteins are summarized regarding their predicted localization in the viral particle in numerical order. The shown intensity represents the mean intensity of all four samples normalized to the mean of all detected glycoproteins. Previously identified proteins are indicated with yes ("Y") or no ("N") (Loret et al., 2008; Russell et al., 2018). "MW" means molecular weight. Proteins detected in two out of three samples are marked with "#."

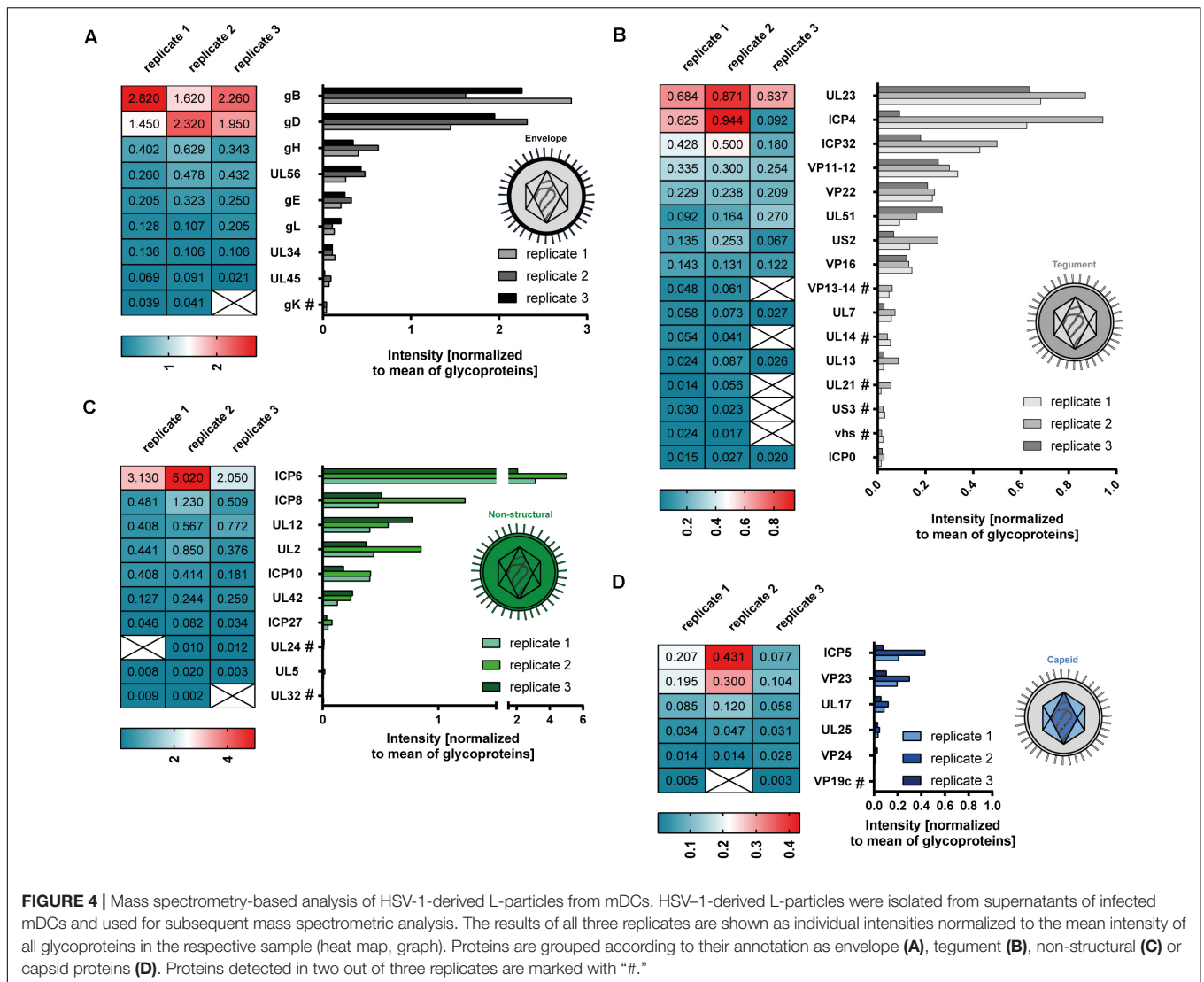


predominantly produce L-particles (Figure 1A), we exclude the possibility of significant H-particle contaminations in our mDCs preparations. Regarding proteins predicted within the tegument, we detected the UL23 as the most abundant protein, which is responsible for the phosphorylation of thymidine and thus the production of nucleotides for viral DNA synthesis (Chen et al., 1998; Pilger et al., 1999; Xie et al., 2019). Furthermore, we detected the viral protein ICP32, which is known as larger inner tegument protein, responsible for cytoplasmic secondary envelopment (Owen et al., 2015). Also the functionally important viral protein VP16, initializing the viral IE gene expression cascade, was identified in these L-particle preparations (Figure 4B; Triezenberg, 1995). Surprisingly, apart from the high abundant HSV-1-encoded proteins gB and gD in L-particles derived from HSV-1-infected mDCs, we

also detected high amounts of ICP6, which is categorized in non-structural proteins. In summary, L-particles produced by HSV-1-infected mDCs are highly coated by the two glycoproteins gB and gD and contain three of the five known IE proteins (ICP0, ICP4, ICP27).

HSV-1-Derived L-Particles Possess a Cell Type-Dependent Unique Protein Signature

For better illustration and comparison between L-particles released by HSV-1-infected BHK21 cells and mDCs, the top three to four abundant proteins for each protein group are schematically depicted in Figure 5. However, L-particles are derived from two different cell types and measurements and

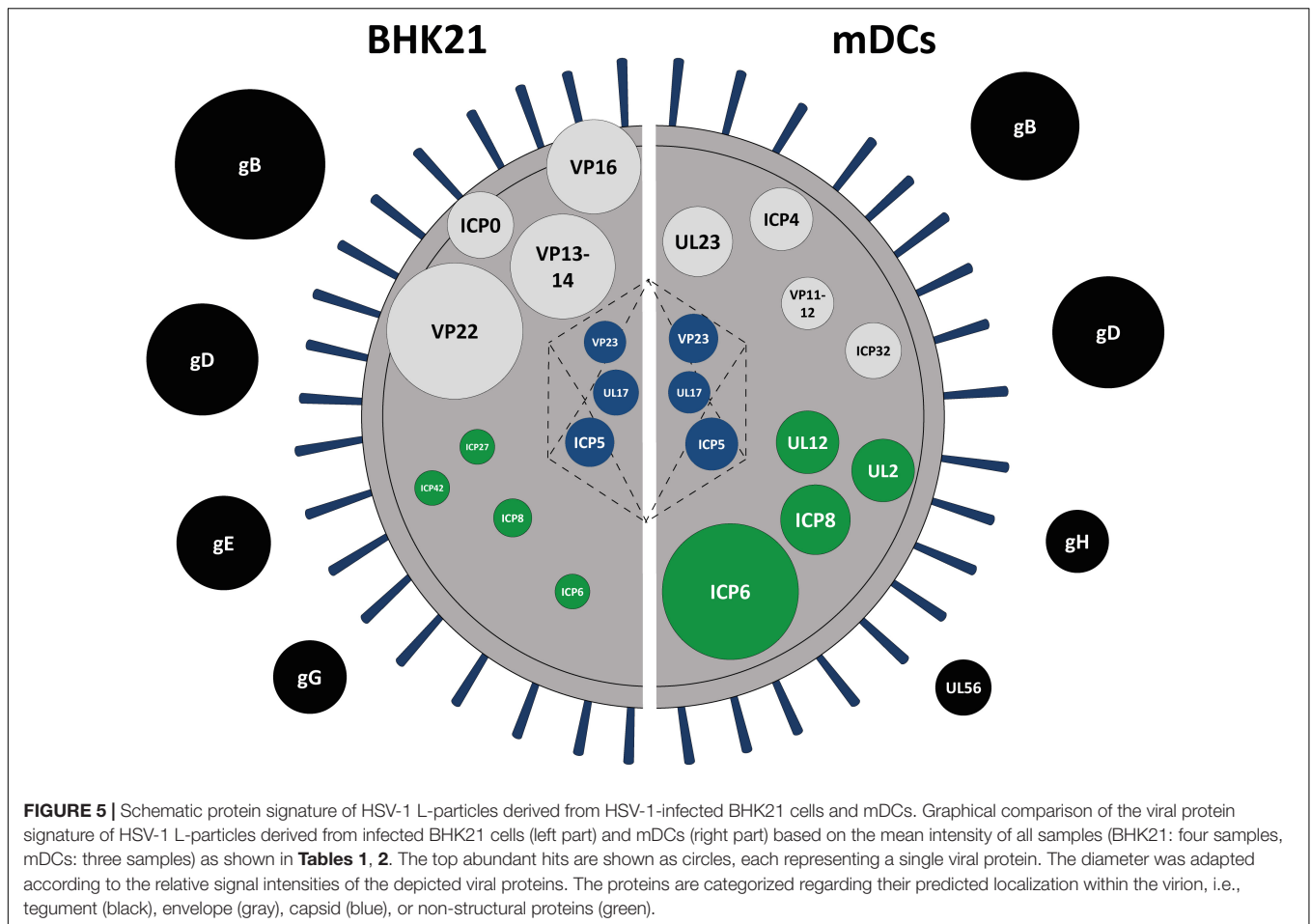


thus the detection of different peptides is not linear. Regarding HSV-1 L-particles derived from either of the two cell types, we revealed that both preparations shared some characteristics, i.e., the presence of particular glycoproteins and non-structural proteins. Especially the high abundancy of gB and gD were comparable in both particle preparations from BHK21 cells and mDCs (Figures 3A, 4A, 5). Even though the intensity of the non-structural proteins strongly differed between L-particles from BHK21 cells and mDCs, the major hits, e.g., ICP6 and ICP8, were identical (Figure 5, green circles). However, the distribution among tegument and capsid proteins was inconsistent between L-particles from BHK21 cells and mDCs. In particular, L-particles from HSV-1-infected BHK21 cells contained high amounts of VP22, VP13-14, ICP0, and VP16 protein, while the major hits in mDC-derived HSV-1 L-particles were UL23, ICP4, VP11-12 and ICP32. Although the capsid and thus the viral genome is not present in L-particles, the major capsid protein ICP5 could, however, in some degree be detected in L-particles derived from HSV-1-infected BHK21 cells as well as mDCs (Figures 3D,

4D, 5). Notwithstanding, it is very likely that capsid proteins are incorporated into L-particles, whereas progeny capsids are absent in this non-infectious HSV-1 particle structure. In conclusion, our data indicate that the composition of HSV-1-derived L-particles is reflected by the producing cell type.

Host Cell Protein Composition in BHK21- and mDC-Derived Particles

Having analyzed the viral protein composition of BHK21cell- and mDC-derived particles, we next investigated host cell protein incorporation in HSV-1 particles. We detected 1,092 (out of 31,693 total protein count in *Mesocricetus auratus*) and 1,762 (out of 74,823 total protein count in *Homo sapiens*) host cell proteins in BHK21 cell-derived and mDC-derived particles, respectively (Figure 6). The detected host cell proteins in BHK21 cell- and mDC-derived HSV-1 particles, as well as the 630 proteins which are found in the particle types from different cell types, are shown in the supplementary section (Supplementary Tables S1–S3).



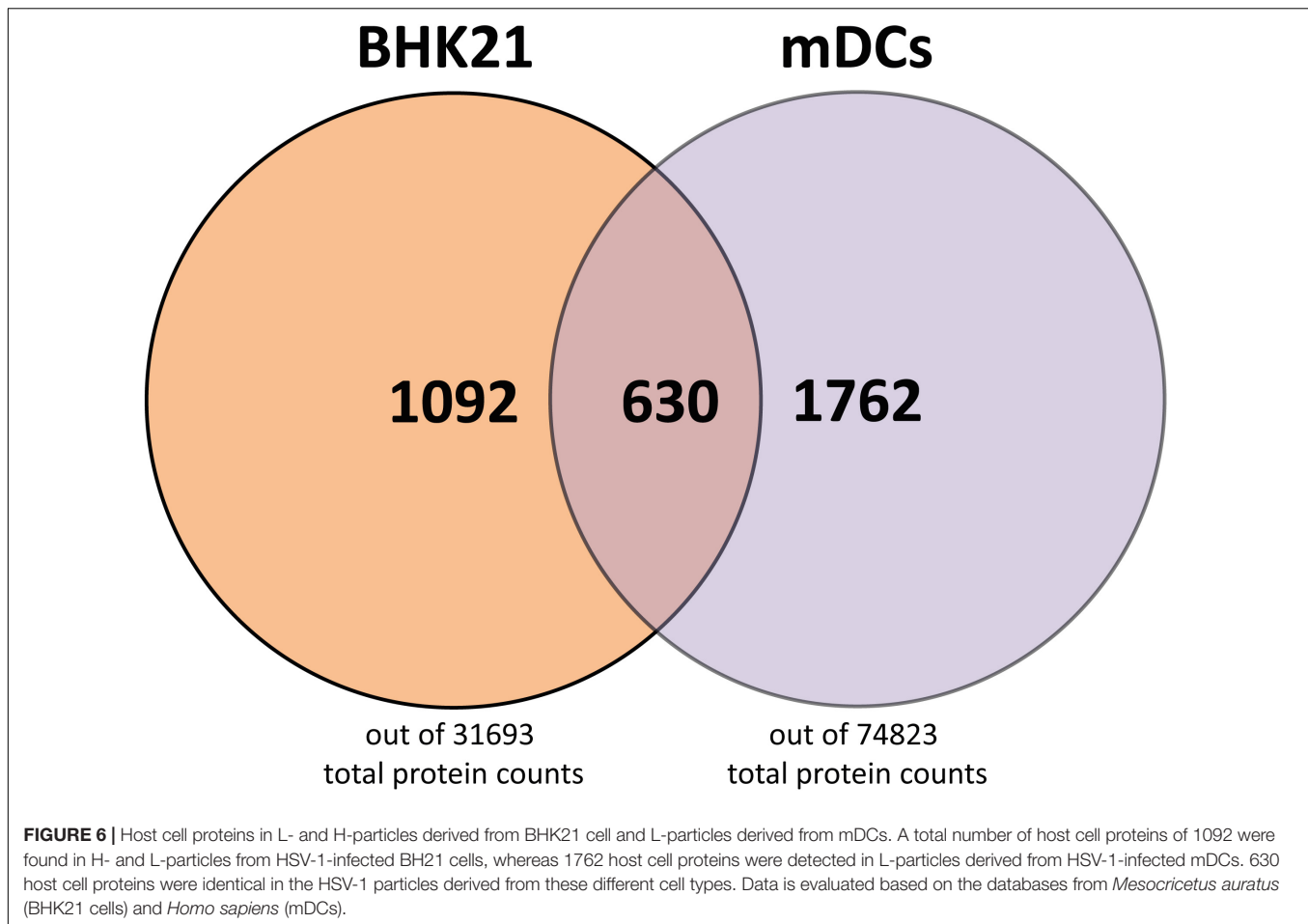
However, the detection of host cell proteins does not allow the conclusion that they are also incorporated into particles, since we cannot exclude small contaminations of extracellular particles.

HSV-1-Derived L-Particles Specifically Modulate CD83 Expression During DC Activation and Inhibit DC T Cell Stimulatory Capacity

L-particles derived from both HSV-1 infected BHK21 cells and mDCs contain a plethora of viral proteins (**Tables 1, 2**). To further analyze the functional role of L-particles during an HSV-1 infection, it was interesting to investigate whether non-infectious particles are able to interfere with DC maturation or with the T cell stimulatory capacity of mDCs.

In humans, the uptake of foreign antigens by iDCs in the periphery causes fundamental changes in their phenotype as well as their migratory behavior (Lanzavecchia and Sallusto, 2001; Alvarez et al., 2008). This process is known as DC maturation, which is pivotal for the ability to stimulate naive T cells. Previous studies revealed that the infection of iDCs with HSV-1 impedes their maturation into antigen presenting mDCs (Salio et al., 1999; Grosche et al., 2020). To investigate the impact of L-particles on DC maturation, iDCs were treated with L-particles, HSV-1

virions or MNT buffer, serving as a control, followed by the addition of a defined DC maturation cocktail. Since L-particles are lacking the viral genome and are replication incompetent, UV-inactivated virions are used as an additional control to prove the effect of viral DNA on the observed phenotype. The immature phenotype of these DCs is characterized by moderate expression levels of CD11c, low expression of the chemokine receptor CCR7, as well as the costimulatory molecule CD80, the functionally important CD83 protein and MHC class II molecules which are important for peptide-antigen presentation (von Rohrscheidt et al., 2016; Duthorn et al., 2019). Upon treatment of iDCs with the maturation cocktail, mock cells efficiently undergo maturation, which was reflected by the upregulation of all analyzed activation surface molecules (**Figure 7**). As previously reported, HSV-1 virions block DC maturation and efficiently inhibit the upregulation of CCR7, MHC class II, CD80 and CD83 (Salio et al., 1999; Grosche et al., 2020). Interestingly, our data demonstrate that L-particles derived from BHK21 cells failed to inhibit the phenotypic maturation of iDCs toward mDCs, since we observed elevated surface expression of CCR7, CD80 and CD11c, comparable to mock-treated controls (**Figure 7**). Also the phenotype of DCs treated with UV-irradiated HSV-1-virions was comparable to the expression pattern of DCs treated with BHK21-derived L-particles, except for the slightly



decreased CCR7 expression. In sharp contrast, L-particles were sufficient to completely hamper CD83 upregulation. Whether L-particles actively mediate the downregulation of CD83 or block the upregulation of this important surface molecule during DC maturation has to be clarified in future studies.

Due to the considerable amount of viral proteins and the above described impairment of CD83 upregulation during maturation of iDCs, it is tempting to speculate that L-particles contribute to efficient HSV-1 replication and/or downmodulation of DC-mediated antiviral immune responses in the human host. For human mDCs, it has been shown *in vitro* that infectious virions reduce the T cell stimulatory capacity of these infected mDCs (Kruse et al., 2000). Therefore, it was of high interest to investigate whether also non-infectious L-particles impair the T cell stimulatory capacity of mDCs. Thus, functional mixed lymphocyte reaction (MLR) assay was performed, using mDCs infected for 8 h either (i) with pure HSV-1 virions (H-particles), treated (ii) with UV-irradiated H-particles or (iii) L-particles (all derived from BHK21 cells), or (iv) MNT buffer as mock control. As shown in **Figure 8** (black line), mock treated mDC very potently induce T cell proliferation. In sharp contrast, mDCs infected with H-particles were almost completely inhibited in their T cell stimulatory capacity (gray line). Noteworthy, and

highly interesting, also mDCs which have been incubated with L-particles derived from BHK21 cells (black dashed line) or UV-inactivated H-particles (blue line) revealed a strongly hampered T cell stimulatory capacity. In conclusion, these functional analyses support our hypothesis that L-particles modulate DC biology and function.

DISCUSSION

During co-evolution, HSV-1 has evolved several immune evasion mechanisms to subvert the host's immune response and to particularly interfere with DC biology and function. Recent experiments showed that nuclear lamin proteins are degraded in HSV-1-infected iDCs via hijacking cellular autophagy, which in turn enables the nuclear egress of viral capsids and pilots the release of full mature virions (Turan et al., 2019). Conversely, in HSV-1-infected mDCs, autophagic flux is inhibited via the upregulation of KIF proteins preventing the nuclear egress of viral capsid. As a result, mainly capsidless L-particles and only marginal amounts of mature virions are released into the supernatants of HSV-1-infected mDCs (**Figure 1A**). However, the production of L-particles is a common process observed among all alpha herpesviruses

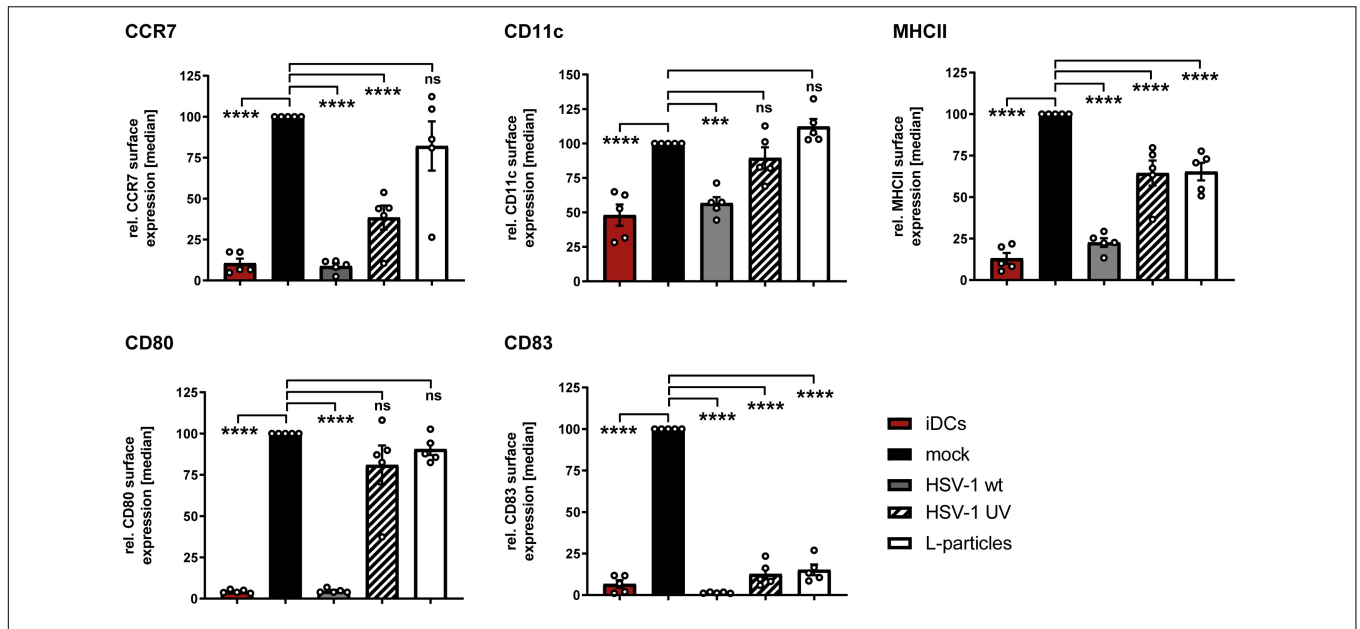


FIGURE 7 | L-particles selectively interfere with CD83 surface expression during DC maturation. Immature DCs (iDCs) were infected with HSV-1 (MOI of 2), treated with UV-inactivated HSV-1 (viral material corresponding to MOI of 20, $8 \times 0.12 \text{ J/cm}^2$) or L-particles (viral material corresponding to high MOI, $3 \times 0.12 \text{ J/cm}^2$) or left untreated. At 1 hpi, infected cells were transferred into medium containing a defined maturation cocktail. An uninfected iDC sample served as an input control and was directly stained against CD11c, CD80, CD83, CCR7, and MHC class II (MHCII) for flow cytometric analyses. Cells were harvested 24 hpi, stained with specific antibodies mentioned before and used for flow cytometry. The experiment was performed five times with cells from different healthy donors. Error bars indicate SEM. Significant changes to mock were analyzed using a one-way ANOVA and Bonferroni multiple comparison *post hoc* tests and are indicated by asterisks (** indicates $p \leq 0.01$ and **** $p \leq 0.0001$) and values depicted as “ns” were not significant ($p < 0.05$).

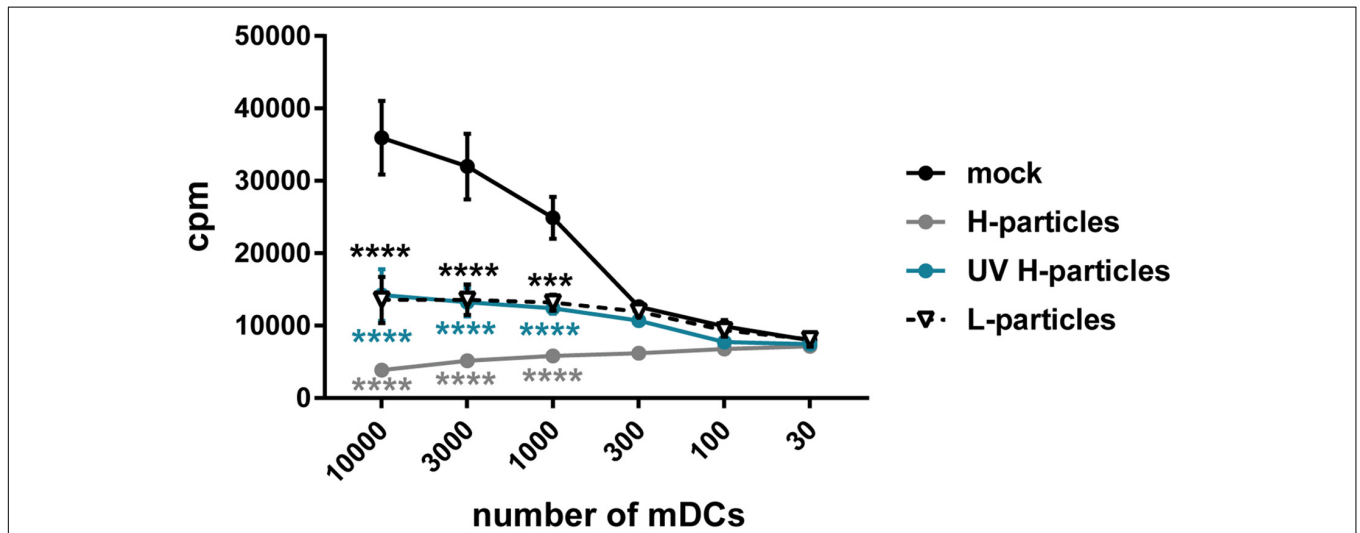


FIGURE 8 | L-particles possess an immunomodulatory effect on mDCs. Mature DCs (mDCs) were infected with purified H-particles (MOI of 2), treated with UV-irradiated H-particles (viral material corresponding to MOI of 20, $8 \times 0.12 \text{ J/cm}^2$) or L-particles (viral material corresponding to high MOI, $3 \times 0.12 \text{ J/cm}^2$) or left untreated (mock). At 8 hpi, cells were cocultured with allogeneic T cells in a mixed lymphocyte reaction (MLR) for additional 72 h. Cells were pulsed with $1 \mu\text{Ci/well}$ [^3H]-thymidine (PerkinElmer) for 16 h before harvesting. The experiment was performed three times with mDCs from different healthy donors. Error bars indicate SEM. Statistical analyses was performed relative to mock values and is depicted on the right side. Only the significant changes to mock were analyzed using a one-way ANOVA and Bonferroni multiple comparison *post hoc* tests and only significant changes are indicated by asterisks (* indicates $p \leq 0.05$, ** $p \leq 0.01$, *** $p \leq 0.001$, and **** $p \leq 0.0001$).

or during the infection of different cell types (Figure 1A; Dargan and Subak-Sharpe, 1997). Since L-particles derived from HSV-1-infected BHK21 cells and mDCs have been described

to affect CD83 surface expression on directly HSV-1-infected and bystander mDCs (Heilingloh et al., 2015), their viral protein composition was analyzed via MS1-based label-free

quantification in the present study. In addition, the role of these L-particles in respect to the functional impairment of DCs was studied in more detail.

In general, our mass spectrometric data regarding H-particles derived from BHK21 cell are comparable to the results previously published by other groups (Loret et al., 2008; Russell et al., 2018). Especially the major hits of the capsid (ICP5, VP23), tegument (VP22, UL47, UL36) and envelope proteins (gB, gD, gE) are similar to those provided by Loret et al. (2008). Concerning the abundancy of gB in the viral envelope or U_S11 in the tegument, previous studies revealed a higher tendency in L-particles compared to H-particles (Russell et al., 2018). The envelope protein gC was almost absent in the H- and L-particle preparations derived from HSV-1-infected BHK21 cells as well as in L-particles derived from mDCs (**Figures 3A, 4A**). As previously published, the virus stock strain 17 syn⁺, which was used in the present study, is heterogenic regarding the gC coding region (Cunha et al., 2015; Jones et al., 2019). This means, that different gC variants are present in the virus stock strain 17 syn⁺. Since some variants miss the transmembrane domain (Jones et al., 2019), this might explain the almost complete absence of gC in our particle preparations. These observations were confirmed by our MS1-based label-free quantification (**Figures 3A,B**). Taken together, we revealed ~86% (63 viral proteins) and ~56% (41 viral proteins) of all annotated viral HSV-1 strain 17 proteins (73 proteins) to be incorporated into HSV-1-derived particles from infected BHK21 cells and mDCs, respectively (UniProt, Reference Proteome, Proteome ID: UP000009294). However, the number of HSV-1-encoded proteins expressed by infected mDCs might differ from that of BHK21 cells.

Since the working group of Loret et al. (2008) reported the NEC components UL31 (NEC1) and UL34 (NEC2) to be absent in mature virions, one of the most surprising result of our mass spectrometry-based approach was the detection of the two NEC components UL31 and UL34 in L-particles derived from BHK21 cells (**Figure 3**), while exclusively UL34 was identified in L-particle preparations from mDCs (**Figure 4**). However, given the normalized signal intensity of UL31 to the mean of all glycoproteins, it appears that this protein is very low-abundant (<1%) in HSV-1-derived particles from BHK21 cells (**Figure 3**). In contrast, UL34 shows a higher normalized average signal intensity in H- and L-particles derived from BHK21 cells, while it is approximately 3.5 times overrepresented in L-particles compared to H-particles. Notably, L-particles derived from HSV-1-infected mDCs showed an equal normalized intensity of incorporated UL34 (**Figure 4**). In contrast to the findings of Loret et al. (2008), and in agreement with our observations, UL34 has been detected in virions of cytoplasmic extracts (Purves et al., 1992). Given the fact, that the production and function of non-infectious L-particles has not been intensively investigated yet, the reason for the higher abundance of UL34 in L-particles compared to H-particles from BHK21 cells requires further substantial investigation.

The HSV-1 tegument-associated proteins ICP0 and ICP4 are two key factors during HSV-1 replication. Both

proteins are not only important modulators of intrinsic and innate immunity (Alandijany, 2019; Tognarelli et al., 2019), but are also crucial during the initiation of the viral gene expression cascade (Guo et al., 2010). On the one hand, it has been suggested that ICP4 might be an L-particle specific viral protein (Szilágyi and Cunningham, 1991; Heilingloh et al., 2015). On the other hand, several studies confirmed the presence of both viral proteins in mature virions (Yao and Courtney, 1989, 1992; Loret et al., 2008; Sedlackova and Rice, 2008; Delboy et al., 2010; Loret and Lippé, 2012; Russell et al., 2018). In line with the latter statement, our mass spectrometric data revealed ICP0 and ICP4 to be present in a comparable amount in L-particles and also in mature virions of HSV-1-infected BHK21 cells (**Figure 3B**). Based on their numerous functions during viral replication or immune evasion mechanisms, we suppose that these two viral proteins are not only virion- but also L-particle-associated components, to shape the microcellular environment for the benefit of the virus (Heilingloh et al., 2015).

Despite the hypothesis that H- and L-particles share a similar way of maturation, the non-infectious particles can also be produced in the absence of DNA replication and packaging (Dargan et al., 1995; Russell et al., 2018). Two important proteins regarding DNA replication are, e.g., ICP8, a single-stranded DNA binding protein (Zhou and Knipe, 2002; Weerasooriya et al., 2019), and the viral thymidine kinase UL23, which phosphorylates thymidine and thus prepares nucleotides for viral DNA synthesis (Chen et al., 1998; Pilger et al., 1999; Xie et al., 2019). Our mass spectrometric data of BHK21 cell-derived HSV-1 particles revealed ICP8 and UL23 to be present in L- and H-particles, representing the major hits among non-structural proteins (**Table 2** and **Figure 3**). Interestingly, the normalized intensity of ICP8 and UL23 in L-particles derived from HSV-1-infected mDCs is extremely higher compared to particle preparations from HSV-1-infected BHK21 cells (**Figures 3, 4**). Since ICP8 is also described to inhibit stress granule formation and therefore prevents innate immune pathways, one possible reason for the presence of this viral protein might be the support of subsequent infection with HSV-1 mature virions and thus promoting viral replication and viral DNA transcription (Panas et al., 2015; Burgess and Mohr, 2018).

In L-particles derived from HSV-1-infected mDCs several proteins were detected counteracting cell death. First, ICP6, as major hit in mDC particles (**Figure 4C**), is an important viral protein for replication, since the ablation of ICP6 results in severe replication defects (Goldstein and Weller, 1988; Mostafa et al., 2018). While HSV-1 ICP6 activates programmed cell necrosis in mice (Huang et al., 2015), this viral protein acts as an inhibitor of cellular apoptosis and prevents the induction of necroptosis in human cells (Dufour et al., 2011; Guo et al., 2015; Yu et al., 2016; Mostafa et al., 2018). Particularly, the expression of both Ribonucleotide Reductase R1 subunits (ICP6 and ICP10) preserves from TNF α - and FasL-induced apoptosis (Dufour et al., 2011). Another protein leading to the blocking

of apoptosis is gD, which is also one of the major hits in mDC-derived L-particles (**Figure 4A**; Zhou et al., 2000; Yu and He, 2016). Thus, it seems that HSV-1 L-particles transfer several proteins that manipulate host cell death to promote viral replication.

Upon an HSV-1 infection, anti-HSV-1 antibodies are generated during adaptive immune responses and are mainly targeted against the glycoproteins gD and gB (Crisuolo et al., 2019), two proteins which are highly expressed on the surface of HSV-1 virions (Cai et al., 1988; Eisenberg et al., 2012). Interestingly, L-particles derived from HSV-1-infected BHK21 cells and mDCs also contain significant amounts of both glycoproteins (**Figures 3A, 4A**). In Hepatitis B virus (HBV) infection, Rydell et al. showed that the presence of capsidless subviral particles diminished the neutralization capacity of anti-HBV antibodies (Rydell et al., 2017). Based on this observation, we suggest that L-particles released during an HSV-1 infection could also intercept antibodies targeted against gB or gD. This hypothesis is further supported by the finding that L-particles are predominantly produced by recently infected cells early after infection and to a lesser extent by cells located inside the center of infection (Alemañ et al., 2003) and thus might capture anti-HSV-1 antibodies prior to the release of infectious virions.

The functional role of L-particles during HSV-1 infection has been rarely investigated during the last years. Previous studies already revealed that infectious HSV-1 virions both hamper the mDC T cell stimulatory (Kruse et al., 2000; Pollara et al., 2003) as well as the iDC maturation capacity (Salio et al., 1999; Grosche et al., 2020). However, L-particles have not been analyzed regarding their impact on these two DC features. During DC maturation, L-particles specifically interfere with CD83 expression and not with any other analyzed maturation marker (**Figure 7**). By contrast to HSV-1-infected mDCs, which are completely inhibited in their T cell stimulatory capacity, L-particle-treated mDCs also show a significantly reduced ability to activate T cells (**Figure 8**). Based on these results, L-particles seem to disturb DC functions and therefore could be released to modulate surrounding bystander cells during HSV-1 infection.

In summary, the here presented comparative analysis extends recent reports regarding the viral protein composition of HSV-1-derived particles. In particular, we detected 63 viral proteins in infectious H- and L-particles from HSV-1-infected BHK21 cells and 41 viral proteins in L-particles from HSV-1-infected mDCs. Our data provide evidence that L-particles derived from HSV-1-infected BHK21 cells or mDCs transfer a plethora of viral proteins from infected cells to uninfected bystander cells. In this regard, we revealed that L-particles possess an immunomodulatory effect on DCs and suppress their T cell stimulatory capacity. Finally, we hypothesize that HSV-1 L-particles are produced and released by infected cells in order to shape and subvert the host's immune response. L-particles not only foster HSV-1 replication via transferring essential viral proteins and modulate vital functions of DCs, but might also be essential for the interception of the host's humoral antiviral immune response.

DATA AVAILABILITY STATEMENT

The MS proteomics data have been deposited to the ProteomeXchange Consortium via the PRIDE partner repository with the data set identifiers PXD020845 (BHK21 particles) and PXD020846 (mDC particles).

ETHICS STATEMENT

The studies involving human participants were reviewed and approved by the "Ethik-Kommission der Friedrich-Alexander-Universität Erlangen-Nürnberg". The patients/patients/participants provided their written informed consent to participate in this study.

AUTHOR CONTRIBUTIONS

AB, LP, and AS designed the project and critically revised the manuscript. AB and PM-Z performed experiments. AB and LP interpreted the data. MK provided essential reagents and performed mass spectrometric measurements. JH performed PEAKS analyses of measurements from BHK21 cell- and mDC-derived particles. CH carried out electron microscopy. AB did formal the data analyses and prepared the original draft manuscript. All authors approved the final version of the manuscript.

FUNDING

This research was supported by the German Research Foundation (Deutsche Forschungsgemeinschaft, DFG), grant number STE 432/11-1, awarded to AS. AB was funded by the ELAN Program (Faculty of Medicine, Friedrich-Alexander-Universität Erlangen-Nürnberg; project 18-12-21-1, awarded to LP. AB was supported by the DFG funded GRK2504.

ACKNOWLEDGMENTS

We acknowledge support within the funding program Open Access Publishing by the Friedrich-Alexander-Universität Erlangen-Nürnberg (FAU).

SUPPLEMENTARY MATERIAL

The Supplementary Material for this article can be found online at: <https://www.frontiersin.org/articles/10.3389/fmicb.2020.01997/full#supplementary-material>

REFERENCES

- Alandijany, T. (2019). Host intrinsic and innate intracellular immunity during herpes simplex Virus Type 1 (HSV-1) Infection. *Front. Microbiol.* 10:2611. doi: 10.3389/fmicb.2019.02611
- Alemañ, N., Quiroga, M. I., López-Peña, M., Vázquez, S., Guerrero, F. H., and Nieto, J. M. (2003). L-particle production during primary replication of pseudorabies virus in the nasal mucosa of swine. *J. Virol.* 77, 5657–5667. doi: 10.1128/jvi.77.10.5657-5667.2003
- Alvarez, D., Vollmann, E. H., and von Andrian, U. H. (2008). Mechanisms and consequences of dendritic cell migration. *Immunity* 29, 325–342. doi: 10.1016/j.immuni.2008.08.006
- Bantscheff, M., Schirle, M., Sweetman, G., Rick, J., and Kuster, B. (2007). Quantitative mass spectrometry in proteomics: a critical review. *Anal. Bioanal. Chem.* 389, 1017–1031. doi: 10.1007/s00216-007-1486-6
- Bigalke, J. M., and Heldwein, E. E. (2017). Have NEC coat, will travel: structural basis of membrane budding during nuclear egress in herpesviruses. *Adv. Virus Res.* 97, 107–141. doi: 10.1016/bs.aivir.2016.07.002
- Burgess, H. M., and Mohr, I. (2018). Defining the role of stress granules in innate immune suppression by the herpes simplex Virus 1 Endoribonuclease VHS. *J. Virol.* 92:e00829-18. doi: 10.1128/jvi.00829-18
- Cai, W. H., Gu, B., and Person, S. (1988). Role of glycoprotein B of herpes simplex virus type 1 in viral entry and cell fusion. *J. Virol.* 62, 2596–2604. doi: 10.1128/jvi.62.8.2596-2604.1988
- Chen, S. H., Cook, W. J., Grove, K. L., and Coen, D. M. (1998). Human thymidine kinase can functionally replace herpes simplex virus type 1 thymidine kinase for viral replication in mouse sensory ganglia and reactivation from latency upon explant. *J. Virol.* 72, 6710–6715. doi: 10.1128/jvi.72.8.6710-6715.1998
- Coffin, R. S., MacLean, A. R., Latchman, D. S., and Brown, S. M. (1996). Gene delivery to the central and peripheral nervous systems of mice using HSV1 ICP34.5 deletion mutant vectors. *Gene Ther.* 3, 886–891.
- Coffin, R. S., Thomas, S. K., Thomas, N. S., Lilley, C. E., Pizzey, A. R., Griffiths, C. H., et al. (1998). Pure populations of transduced primary human cells can be produced using GFP expressing herpes virus vectors and flow cytometry. *Gene Ther.* 5, 718–722. doi: 10.1038/sj.gt.3300634
- Crisuolo, E., Castelli, M., Diotti, R. A., Amato, V., Burioni, R., Clementi, M., et al. (2019). Cell-to-cell spread blocking activity is extremely limited in the sera of herpes simplex Virus 1 (HSV-1)- and HSV-2-Infected subjects. *J. Virol.* 93:e00070-19. doi: 10.1128/jvi.00070-19
- Crump, C. (2018). Virus Assembly and Egress of HSV. *Adv. Exp. Med. Biol.* 1045, 23–44. doi: 10.1007/978-981-10-7230-7_2
- Cunha, C. W., Taylor, K. E., Pritchard, S. M., Delboy, M. G., Komala Sari, T., Aguilar, H. C., et al. (2015). Widely Used Herpes Simplex Virus 1 ICP0 Deletion Mutant Strain dl1403 and Its Derivative Viruses Do Not Express Glycoprotein C Due to a Secondary Mutation in the gC Gene. *PLoS One* 10:e0131129. doi: 10.1371/journal.pone.0131129
- Dargan, D. J., Patel, A. H., and Subak-Sharpe, J. H. (1995). PREPs: herpes simplex virus type 1-specific particles produced by infected cells when viral DNA replication is blocked. *J. Virol.* 69, 4924–4932. doi: 10.1128/jvi.69.8.4924-4932.1995
- Dargan, D. J., and Subak-Sharpe, J. H. (1997). The effect of herpes simplex virus type 1 L-particles on virus entry, replication, and the infectivity of naked herpesvirus DNA. *Virology* 239, 378–388. doi: 10.1006/viro.1997.8893
- Dauber, B., Saffran, H. A., and Smiley, J. R. (2014). The herpes simplex virus 1 virion host shutoff protein enhances translation of viral late mRNAs by preventing mRNA overload. *J. Virol.* 88, 9624–9632. doi: 10.1128/jvi.01350-14
- Delboy, M. G., Siekavizza-Robles, C. R., and Nicola, A. V. (2010). Herpes simplex virus tegument ICP0 is capsid associated, and its E3 ubiquitin ligase domain is important for incorporation into virions. *J. Virol.* 84, 1637–1640. doi: 10.1128/jvi.02041-09
- Dufour, F., Sasseville, A. M., Chabaud, S., Massie, B., Siegel, R. M., and Langelier, Y. (2011). The ribonucleotide reductase R1 subunits of herpes simplex virus types 1 and 2 protect cells against TNF α - and FasL-induced apoptosis by interacting with caspase-8. *Apoptosis* 16, 256–271. doi: 10.1007/s10495-010-0560-2
- Düthorn, A., Turan, A., Drassner, C., Mühl-Zürbes, P., Heilingloh, C. S., Steinkasserer, A., et al. (2019). siRNA electroporation to modulate autophagy in herpes simplex virus type 1-infected monocyte-derived Dendritic Cells*. *J. Vis. Exp.* doi: 10.3791/60190
- Eisenberg, R. J., Atanasiu, D., Cairns, T. M., Gallagher, J. R., Krummenacher, C., and Cohen, G. H. (2012). Herpes virus fusion and entry: a story with many characters. *Viruses* 4, 800–832. doi: 10.3390/v4050800
- Goldstein, D. J., and Weller, S. K. (1988). Factor(s) present in herpes simplex virus type 1-infected cells can compensate for the loss of the large subunit of the viral ribonucleotide reductase: characterization of an ICP6 deletion mutant. *Virology* 166, 41–51. doi: 10.1016/0042-6822(88)90144-4
- Goldwich, A., Prectel, A. T., Mühl-Zürbes, P., Pangratz, N. M., Stössel, H., Romani, N., et al. (2011). Herpes simplex virus type 1 (HSV-1) replicates in mature dendritic cells but can only be transferred in a cell-cell contact-dependent manner. *J. Leukoc Biol.* 89, 973–979. doi: 10.1189/jlb.0310180
- Granzow, H., Klupp, B. G., Fuchs, W., Veits, J., Osterrieder, N., and Mettenleiter, T. C. (2001). Egress of alphaherpesviruses: comparative ultrastructural study. *J. Virol.* 75, 3675–3684. doi: 10.1128/jvi.75.8.3675-3684.2001
- Grosche, L., Döhner, K., Dühorn, A., Hickford-Martinez, A., Steinkasserer, A., and Sodeik, B. (2019). Herpes simplex virus type 1 propagation, titration and single-step growth curves. *Bio-protocol* 9:e3441. doi: 10.21769/BioProtoc.3441
- Grosche, L., Mühl-Zürbes, P., Ciblis, B., Krawczyk, A., Kuhnt, C., Kamm, L., et al. (2020). Herpes simplex virus type-2 paralyzes the function of monocyte-derived dendritic cells*. *Viruses* 12:112. doi: 10.3390/v12010112
- Guo, H., Omoto, S., Harris, P. A., Finger, J. N., Bertin, J., Gough, P. J., et al. (2015). Herpes simplex virus suppresses necroptosis in human cells. *Cell Host Microbe* 17, 243–251. doi: 10.1016/j.chom.2015.01.003
- Guo, H., Shen, S., Wang, L., and Deng, H. (2010). Role of tegument proteins in herpesvirus assembly and egress. *Protein Cell* 1, 987–998. doi: 10.1007/s13238-010-0120-0
- Heilingloh, C. S., and Krawczyk, A. (2017). Role of L-particles during herpes simplex virus infection. *Front. Microbiol.* 8:2565. doi: 10.3389/fmicb.2017.02565
- Heilingloh, C. S., Kummer, M., Mühl-Zürbes, P., Drassner, C., Daniel, C., Klewer, M., et al. (2015). L particles transmit viral proteins from herpes simplex virus 1-infected mature dendritic cells to uninfected bystander cells, inducing CD83 downmodulation. *J. Virol.* 89, 11046–11055. doi: 10.1128/jvi.01517-15
- Henaff, D., Remillard-Labrosse, G., Loret, S., and Lippe, R. (2013). Analysis of the early steps of herpes simplex virus 1 capsid tegumentation. *J. Virol.* 87, 4895–4906. doi: 10.1128/jvi.03292-12
- Hogue, I. B., Scherer, J., and Enquist, L. W. (2016). Exocytosis of alphaherpesvirus virions, light particles, and glycoproteins uses constitutive secretory mechanisms. *mBio* 7:e00820-16. doi: 10.1128/mBio.00820-16
- Huang, Z., Wu, S. Q., Liang, Y., Zhou, X., Chen, W., Li, L., et al. (2015). RIP1/RIP3 binding to HSV-1 ICP6 initiates necroptosis to restrict virus propagation in mice. *Cell Host Microbe* 17, 229–242. doi: 10.1016/j.chom.2015.01.002
- Ibiricu, I., Maurer, U. E., and Grünewald, K. (2013). Characterization of herpes simplex virus type 1 L-particle assembly and egress in hippocampal neurons by electron cryo-tomography. *Cell Microbiol.* 15, 285–291. doi: 10.1111/cmi.12093
- Johnson, D. C., and Baines, J. D. (2011). Herpesviruses remodel host membranes for virus egress. *Nat. Rev. Microbiol.* 9, 382–394. doi: 10.1038/nrmicro2559
- Jones, J., Depledge, D. P., Breuer, J., Ebert-Keel, K., and Elliott, G. (2019). Genetic and phenotypic intrastrain variation in herpes simplex virus type 1 Glasgow strain 17 syn+-derived viruses. *J. Gen. Virol.* 100, 1701–1713. doi: 10.1099/jgv.0001343
- Karasneh, G. A., and Shukla, D. (2011). Herpes simplex virus infects most cell types in vitro: clues to its success. *Virol. J.* 8:481. doi: 10.1186/1743-422x-8-481
- Kraner, M. E., Müller, C., and Sonnewald, U. (2017). Comparative proteomic profiling of the choline transporter-like1 (CHER1) mutant provides insights into plasmodesmata composition of fully developed Arabidopsis thaliana leaves. *Plant J.* 92, 696–709. doi: 10.1111/tbj.13702
- Kruse, M., Posorius, O., Krätzer, F., Stelz, G., Kuhnt, C., Schuler, G., et al. (2000). Mature dendritic cells infected with herpes simplex virus type 1 exhibit inhibited T-cell stimulatory capacity. *J. Virol.* 74, 7127–7136. doi: 10.1128/jvi.74.15.7127-7136.2000
- Laine, R. F., Albecka, A., van de Linde, S., Rees, E. J., Crump, C. M., and Kaminski, C. F. (2015). Structural analysis of herpes simplex virus by optical super-resolution imaging. *Nat. Commun.* 6:5980. doi: 10.1038/ncomms6980
- Lamm, C. E., Kraner, M. E., Hofmann, J., Börnke, F., Mock, H.-P., and Sonnewald, U. (2017). Hop/Sti1 – a two-faced cochaperone involved in pattern recognition receptor maturation and viral infection. *Front. Plant Sci.* 8:1754. doi: 10.3389/fpls.2017.01754

- Lanzavecchia, A., and Sallusto, F. (2001). Regulation of T cell immunity by dendritic cells. *Cell* 106, 263–266. doi: 10.1016/s0092-8674(01)00455-x
- Loret, S., Guay, G., and Lippé, R. (2008). Comprehensive characterization of extracellular herpes simplex virus type 1 virions. *J. Virol.* 82, 8605–8618. doi: 10.1128/jvi.00904-08
- Loret, S., and Lippé, R. (2012). Biochemical analysis of infected cell polypeptide (ICP)0, ICP4, UL7 and UL23 incorporated into extracellular herpes simplex virus type 1 virions. *J. Gen. Virol.* 93(Pt 3), 624–634. doi: 10.1099/vir.0.039776-0
- Lv, Y., Zhou, S., Gao, S., and Deng, H. (2019). Remodeling of host membranes during herpesvirus assembly and egress. *Protein Cell* 10, 315–326. doi: 10.1007/s13238-018-0577-9
- McLauchlan, J., Addison, C., Craigie, M. C., and Rixon, F. J. (1992). Noninfectious L-particles supply functions which can facilitate infection by HSV-1. *Virology* 190, 682–688. doi: 10.1016/0042-6822(92)90906-6
- McLauchlan, J., and Rixon, F. J. (1992). Characterization of enveloped tegument structures (L particles) produced by alphaherpesviruses: integrity of the tegument does not depend on the presence of capsid or envelope. *J. Gen. Virol.* 73(Pt 2), 269–276. doi: 10.1099/0022-1317-73-2-269
- McNab, A. R., Desai, P., Person, S., Roof, L. L., Thomsen, D. R., Newcomb, W. W., et al. (1998). The product of the herpes simplex virus type 1 UL25 gene is required for encapsidation but not for cleavage of replicated viral DNA. *J. Virol.* 72, 1060–1070. doi: 10.1128/jvi.72.2.1060-1070.1998
- Mettenleiter, T. C. (2002). Herpesvirus assembly and egress. *J. Virol.* 76, 1537–1547. doi: 10.1128/JVI.76.4.1537-1547.2002
- Mikloska, Z., Bosnjak, L., and Cunningham, A. L. (2001). Immature monocyte-derived dendritic cells are productively infected with herpes simplex virus type 1. *J. Virol.* 75, 5958–5964. doi: 10.1128/JVI.75.13.5958-5964.2001
- Mostafa, H. H., Thompson, T. W., Konen, A. J., Haenchen, S. D., Hilliard, J. G., Macdonald, S. J., et al. (2018). Herpes Simplex Virus 1 Mutant with Point Mutations in UL39 Is Impaired for Acute Viral Replication in Mice, Establishment of Latency, and Explant-Induced Reactivation. *J. Virol.* 92:e01654-17. doi: 10.1128/jvi.01654-17
- Newcomb, W. W., Juhas, R. M., Thomsen, D. R., Homa, F. L., Burch, A. D., Weller, S. K., et al. (2001). The UL6 gene product forms the portal for entry of DNA into the herpes simplex virus capsid. *J. Virol.* 75, 10923–10932. doi: 10.1128/jvi.75.22.10923-10932.2001
- Owen, D. J., Crump, C. M., and Graham, S. C. (2015). Tegument assembly and secondary envelopment of alphaherpesviruses. *Viruses* 7, 5084–5114. doi: 10.3390/v7092861
- Panas, M. D., Schulte, T., Thaa, B., Sandalova, T., Kedersha, N., Achour, A., et al. (2015). Viral and cellular proteins containing FGDF motifs bind G3BP to block stress granule formation. *PLoS Pathog.* 11:e1004659. doi: 10.1371/journal.ppat.1004659
- Pappireddi, N., Martin, L., and Wühr, M. (2019). A review on quantitative multiplexed proteomics. *Chembiochem* 20, 1210–1224. doi: 10.1002/cbic.201800650
- Pfeiffer, I. A., Zinser, E., Strasser, E., Stein, M. F., Dörrie, J., Schaft, N., et al. (2013). Leukoreduction system chambers are an efficient, valid, and economic source of functional monocyte-derived dendritic cells and lymphocytes. *Immunobiology* 218, 1392–1401. doi: 10.1016/j.imbio.2013.07.005
- Pilger, B. D., Perozzo, R., Alber, F., Wurth, C., Folkers, G., and Scapozza, L. (1999). Substrate diversity of herpes simplex virus thymidine kinase. Impact Of the kinematics of the enzyme. *J. Biol. Chem.* 274, 31967–31973. doi: 10.1074/jbc.274.45.31967
- Pollara, G., Speidel, K., Samady, L., Rajpopat, M., McGrath, Y., Lederemann, J., et al. (2003). Herpes simplex virus infection of dendritic cells: balance among activation, inhibition, and immunity. *J. Infect. Dis.* 187, 165–178. doi: 10.1086/367675
- Prechtel, A. T., Turza, N. M., Kobelt, D. J., Eisemann, J. I., Coffin, R. S., McGrath, Y., et al. (2005). Infection of mature dendritic cells with herpes simplex virus type 1 dramatically reduces lymphoid chemokine-mediated migration. *J. Gen. Virol.* 86(Pt 6), 1645–1657. doi: 10.1099/vir.0.80852-0
- Purves, F. C., Spector, D., and Roizman, B. (1992). UL34, the target of the herpes simplex virus U(S)3 protein kinase, is a membrane protein which in its unphosphorylated state associates with novel phosphoproteins. *J. Virol.* 66, 4295–4303. doi: 10.1128/jvi.66.7.4295-4303.1992
- Reynolds, A. E., Wills, E. G., Roller, R. J., Ryckman, B. J., and Baines, J. D. (2002). Ultrastructural Localization of the Herpes Simplex Virus Type 1 UL31, UL34, and US3 Proteins Suggests Specific Roles in Primary Envelopment and Egress of Nucleocapsids. *J. Virol.* 76, 8939–8952. doi: 10.1128/jvi.76.17.8939-8952.2002
- Russell, T., Bleasdale, B., Hollinshead, M., and Elliott, G. (2018). Qualitative Differences in Capsidless L-Particles Released as a By-Product of Bovine Herpesvirus 1 and Herpes Simplex Virus 1 Infections. *J. Virol.* 92:e01259-18. doi: 10.1128/JVI.01259-18
- Rydell, G. E., Prakash, K., Norder, H., and Lindh, M. (2017). Hepatitis B surface antigen on subviral particles reduces the neutralizing effect of anti-HBs antibodies on hepatitis B viral particles in vitro. *Virology* 509, 67–70. doi: 10.1016/j.virol.2017.05.017
- Salio, M., Cella, M., Suter, M., and Lanzavecchia, A. (1999). Inhibition of dendritic cell maturation by herpes simplex virus. *Eur. J. Immunol.* 29, 3245–3253. doi: 10.1002/(sici)1521-4141(199910)29:10<3245::aid-immu3245>3.0.co;2-x
- Salmon, B., Cunningham, C., Davison, A. J., Harris, W. J., and Baines, J. D. (1998). The herpes simplex virus type 1 U(L)17 gene encodes virion tegument proteins that are required for cleavage and packaging of viral DNA. *J. Virol.* 72, 3779–3788. doi: 10.1128/jvi.72.5.3779-3788.1998
- Schleiss, M. R. (2009). Persistent and recurring viral infections: the human herpesviruses. *Curr. Probl. Pediatr. Adolesc. Health Care* 39, 7–23. doi: 10.1016/j.cppeds.2008.10.003
- Sedlackova, L., and Rice, S. A. (2008). Herpes simplex virus type 1 immediate-early protein ICP27 is required for efficient incorporation of ICP0 and ICP4 into virions. *J. Virol.* 82, 268–277. doi: 10.1128/jvi.01588-07
- Smiley, M. L., Hoxie, J. A., and Friedman, H. M. (1985). Herpes simplex virus type 1 infection of endothelial, epithelial, and fibroblast cells induces a receptor for C3b. *J. Immunol.* 134, 2673–2678.
- Szilágyi, J. F., and Cunningham, C. (1991). Identification and characterization of a novel non-infectious herpes simplex virus-related particle. *J. Gen. Virol.* 72(Pt 3), 661–668. doi: 10.1099/0022-1317-72-3-661
- Taddeo, B., Zhang, W., and Roizman, B. (2010). Role of herpes simplex virus ICP27 in the degradation of mRNA by virion host shutoff RNase. *J. Virol.* 84, 10182–10190. doi: 10.1128/jvi.00975-10
- Theodoridis, A. A., Eich, C., Figdor, C. G., and Steinkasserer, A. (2011). Infection of dendritic cells with herpes simplex virus type 1 induces rapid degradation of CYTIP, thereby modulating adhesion and migration. *Blood* 118, 107–115. doi: 10.1182/blood-2010-07-294363
- Thurlow, J. K., Rixon, F. J., Murphy, M., Targett-Adams, P., Hughes, M., and Preston, V. G. (2005). The herpes simplex virus type 1 DNA packaging protein UL17 is a virion protein that is present in both the capsid and the tegument compartments. *J. Virol.* 79, 150–158. doi: 10.1128/jvi.79.1.150-158.2005
- Tognarelli, E. I., Palomino, T. F., Corrales, N., Bueno, S. M., Kalergis, A. M., and González, P. A. (2019). Herpes simplex virus evasion of early host antiviral responses. *Front. Cell Infect. Microbiol.* 9:127. doi: 10.3389/fcimb.2019.00127
- Toropova, K., Huffman, J. B., Homa, F. L., and Conway, J. F. (2011). The herpes simplex virus 1 UL17 protein is the second constituent of the capsid vertex-specific component required for DNA packaging and retention. *J. Virol.* 85, 7513–7522. doi: 10.1128/jvi.00837-11
- Triezenberg, S. J. (1995). Structure and function of transcriptional activation domains. *Curr. Opin. Genet. Dev.* 5, 190–196. doi: 10.1016/0959-437x(95)80007-7
- Trus, B. L., Cheng, N., Newcomb, W. W., Homa, F. L., Brown, J. C., and Steven, A. C. (2004). Structure and polymorphism of the UL6 portal protein of herpes simplex virus type 1. *J. Virol.* 78, 12668–12671. doi: 10.1128/jvi.78.22.12668-12671.2004
- Turan, A., Grosche, L., Krawczyk, A., Mühl-Zürbes, P., Drassner, C., Dühren, A., et al. (2019). Autophagic degradation of lamins facilitates the nuclear egress of herpes simplex virus type 1. *J. Cell Biol.* 218, 508–523. doi: 10.1083/jcb.201801151
- Vittone, V., Diefenbach, E., Triffett, D., Douglas, M. W., Cunningham, A. L., and Diefenbach, R. J. (2005). Determination of interactions between tegument proteins of herpes simplex virus type 1. *J. Virol.* 79, 9566–9571. doi: 10.1128/jvi.79.15.9566-9571.2005
- von Rohrscheidt, J., Petrozziello, E., Nedjic, J., Federle, C., Krzyzak, L., Ploegh, H. L., et al. (2016). Thymic CD4 T cell selection requires attenuation of March8-mediated MHCII turnover in cortical epithelial cells through CD83. *J. Exp. Med.* 213, 1685–1694. doi: 10.1084/jem.20160316

- Watson, G., Xu, W., Reed, A., Babra, B., Putman, T., Wick, E., et al. (2012). Sequence and comparative analysis of the genome of HSV-1 strain McKrae. *Virology* 433, 528–537. doi: 10.1016/j.virol.2012.08.043
- Weerasooriya, S., DiScipio, K. A., Darwish, A. S., Bai, P., and Weller, S. K. (2019). Herpes simplex virus 1 ICP8 mutant lacking annealing activity is deficient for viral DNA replication. *Proc. Natl. Acad. Sci. U.S.A.* 116, 1033–1042. doi: 10.1073/pnas.1817642116
- Whitley, R. J., and Griffiths, P. D. (2002). “Chapter 6 - herpesviruses: an introduction with a focus of herpes simplex virus,” in *Practical Guidelines in Antiviral Therapy*, eds G.J. Galasso, C.A.B. Boucher, D.A. Cooper, D.A. Katzenstein (Amsterdam: Elsevier Science).
- Wiśniewski, J. R., Zougman, A., Nagaraj, N., and Mann, M. (2009). Universal sample preparation method for proteome analysis. *Nat. Methods* 6, 359–362. doi: 10.1038/nmeth.1322
- Xie, Y., Wu, L., Wang, M., Cheng, A., Yang, Q., Wu, Y., et al. (2019). Alpha-herpesvirus thymidine kinase genes mediate viral virulence and are potential therapeutic targets. *Front. Microbiol.* 10:941. doi: 10.3389/fmicb.2019.00941
- Yao, F., and Courtney, R. J. (1989). A major transcriptional regulatory protein (ICP4) of herpes simplex virus type 1 is associated with purified virions. *J. Virol.* 63, 3338–3344. doi: 10.1128/jvi.63.8.3338-3344.1989
- Yao, F., and Courtney, R. J. (1992). Association of ICP0 but not ICP27 with purified virions of herpes simplex virus type 1. *J. Virol.* 66, 2709–2716. doi: 10.1128/jvi.66.5.2709-2716.1992
- Yu, X., and He, S. (2016). The interplay between human herpes simplex virus infection and the apoptosis and necroptosis cell death pathways. *Virol. J.* 13:77. doi: 10.1186/s12985-016-0528-0
- Yu, X., Li, Y., Chen, Q., Su, C., Zhang, Z., Yang, C., et al. (2016). Herpes Simplex Virus 1 (HSV-1) and HSV-2 mediate species-specific modulations of programmed necrosis through the viral ribonucleotide reductase large subunit R1. *J. Virol.* 90, 1088–1095. doi: 10.1128/jvi.02446-15
- Zhang, J., Xin, L., Shan, B., Chen, W., Xie, M., Yuen, D., et al. (2012). PEAKS DB: de novo sequencing assisted database search for sensitive and accurate peptide identification. *Mol. Cell Proteom.* 11:M111.010587. doi: 10.1074/mcp.M111.010587
- Zhou, C., and Knipe, D. M. (2002). Association of herpes simplex virus type 1 ICP8 and ICP27 proteins with cellular RNA polymerase II holoenzyme. *J. Virol.* 76, 5893–5904. doi: 10.1128/jvi.76.12.5893-5904.2002
- Zhou, G., Galvan, V., Campadelli-Fiume, G., and Roizman, B. (2000). Glycoprotein D or J delivered in trans blocks apoptosis in SK-N-SH cells induced by a herpes simplex virus 1 mutant lacking intact genes expressing both glycoproteins. *J. Virol.* 74, 11782–11791. doi: 10.1128/jvi.74.24.11782-11791.2000

Conflict of Interest: The authors declare that the research was conducted in the absence of any commercial or financial relationships that could be construed as a potential conflict of interest.

Copyright © 2020 Birzer, Kraner, Heilingloh, Mühl-Zürbes, Hofmann, Steinkasserer and Popella. This is an open-access article distributed under the terms of the Creative Commons Attribution License (CC BY). The use, distribution or reproduction in other forums is permitted, provided the original author(s) and the copyright owner(s) are credited and that the original publication in this journal is cited, in accordance with accepted academic practice. No use, distribution or reproduction is permitted which does not comply with these terms.